Accepted Manuscript

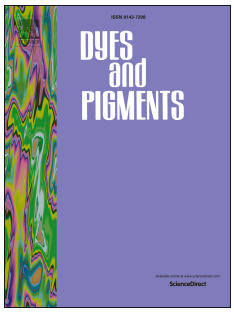

New blue fluorescent and highly thermostable polyimide and poly(amide-imide)s containing triphenylamine units and (4-dimethylaminophenyl)-1,3,4-oxadiazole side groups

Corneliu Hamciuc, Elena Hamciuc, Mihaela Homocianu, Alina Nicolescu, Gabriela Lisa

PII: S0143-7208(17)31210-X

DOI: 10.1016/j.dyepig.2017.09.010

Reference: DYPI 6234

To appear in: *Dyes and Pigments*

Received Date: 27 May 2017

Revised Date: 5 September 2017

Accepted Date: 6 September 2017

Please cite this article as: Hamciuc C, Hamciuc E, Homocianu M, Nicolescu A, Lisa G, New blue fluorescent and highly thermostable polyimide and poly(amide-imide)s containing triphenylamine units and (4-dimethylaminophenyl)-1,3,4-oxadiazole side groups, *Dyes and Pigments* (2017), doi: 10.1016/j.dyepig.2017.09.010.

Graphical Abstract

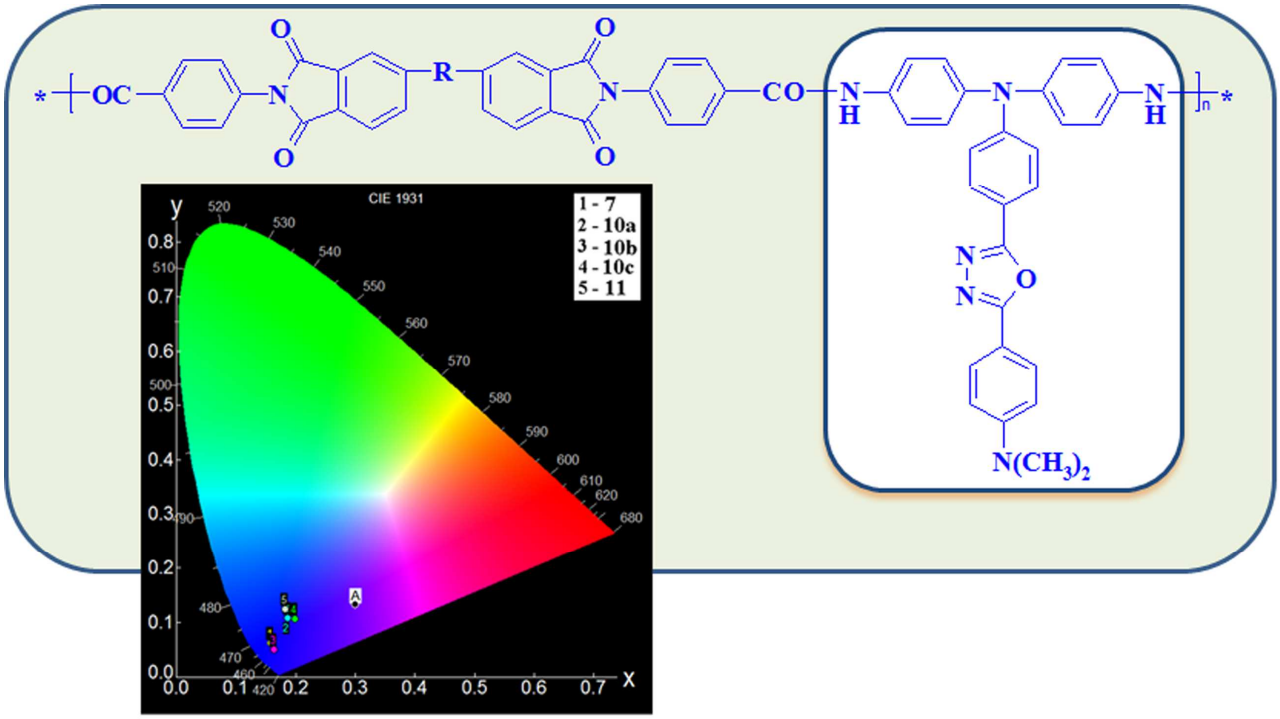

New blue fluorescent and highly thermostable polyimide and poly(amide-imide)s containing triphenylamine units and (4-dimethylaminophenyl)-1,3,4-oxadiazole side groups

Corneliu Hamciuc[*1], Elena Hamciuc[1], Mihaela Homocianu[1], Alina Nicolescu[1], Gabriela Lisa[2]

[1]"Petru Poni" Institute of Macromolecular Chemistry, 41A Aleea Gr. Ghica Voda, 700487 Iasi, Romania

[2]"Gheorghe Asachi" Technical University of Iasi, Faculty of Chemical Engineering and Environmental Protection, Department of Chemical Engineering, 73 D. Mangeron Street, Iasi, Romania

Abstract: A new blue fluorescent aromatic diamine, 2-(4,4′-diamino-4″-triphenylamine)-5-(4-dimethylaminophenyl)-1,3,4-oxadiazole, is synthesized in several steps. Based on this diamine four fluorescent imide-type polymers, a polyimide and three poly(amide-imide)s, are prepared by solution polycondensation reactions. The structures of the monomers and polymers are characterized by FTIR and NMR spectroscopy. The polymers show good solubility in organic solvents, and have high thermal stability, the decomposition temperature being above 380°C, as is determined by TGA measurements. The thermal degradation mechanism of a polymer in an inert atmosphere is investigated by using the coupled TG/MS/FTIR technique. The optical properties are determined by UV-vis and fluorescence spectroscopy. The polymers exhibit strong absorption bands in the range of 357-373 nm, and blue fluorescence in solution within the range of 423-469 nm with low to moderate quantum fluorescence yields from 0.11 to 1.30% and Stokes shifts values of around 77 nm. The protonation is found to affect the spectral properties of the polymers.

[*]Corresponding author
Telephone and Fax: +40 - 232 217454
E-mail address: chamciuc@icmpp.ro (Corneliu Hamciuc)

Keywords: polyimides; 1,3,4-oxadiazole; high thermal stability; blue fluorescence; protonation

1. Introduction

Fully aromatic polyimides are one of the most important classes of high performance polymers used in many applications requiring polymer materials with high temperature resistance. These polymers are characterized by an excellent combination of properties. They exhibit high thermal and thermo-oxidative stability, good mechanical properties and low dielectric constant [1-3]. The main disadvantage of aromatic polyimides is their infusibility and insolubility in organic solvents which make them more difficult to be processed, thus limiting their field of applications. Much research effort has been expended to increase the processability of these polymers, for example by introducing flexible or bulky groups into their macromolecular chains [4, 5]. The presence of amide groups in the polymer chains of an aromatic polyimide leads to a class of polymers, aromatic poly(amide-imide)s, which exhibit a reasonable high thermal stability and show improved solubility in organic solvents and lower glass transition temperatures in comparison with aromatic polyimides of analogous chemical structure [6-8].

The incorporation of hexafluoroisopropylidene (6F) groups or dimethylsilane units produces a disruption of the crystallinity and conjugation of aromatic polyimides. These bulky groups limit the chain packing of the polymers and increase the free volume thus decreasing the dielectric constant. The 6F groups improve considerably flame and oxidation resistance, optical transparency and solubility in organic solvents and decrease the crystallinity, dielectric constant, water absorption and color [9-12]. Also, the presence of dimethylsilane units enhances substantially the solubility in organic solvents and maintains a high thermal stability thus improving the processability of the resulting polymers. It was shown that the introducing of silicon linked through *para* positions of phenylene rings in the main chain gives a σ-π conjugation and allows the transport of electrons [13, 14]. Another way to improve the solubility of the polyimides is the introduction in their main chain

of triphenylamine groups. Such polymers exhibit special optical characteristics and hole-transport properties and can be used in multilayer organic electroluminescent devices [15].

Much research has been directed toward studying blue light-emitting polymer materials with emission efficiency, good thermal stability and high glass transition temperature. One approach to develop such structures is the introduction of blue light-emitting fluorophores in the main or side chains of the polymers. The development of thermostable polyimides having blue-fluorescence properties for applications in light-emitting diodes is of particular interest [16]. These polymers exhibit high glass transition temperature and good thermal and chemical stability. The presence of 1,3,4-oxadiazole rings in the macromolecular chains of the polymers improves the thermal and thermo-oxidative stability, hydrolytic resistance and mechanical properties [17]. Due to the electron-withdrawing character of the 1,3,4-oxadiazole ring, several oxadiazole-containing polymers were studied for the construction of organic light-emitting diodes [18]. It is known that the polymers with electron donor dimethylamino substituents in the *para*-position of the pendant chromophoric 2,5-diphenyl-1,3,4-oxadiazole unit are promising candidates for emissive materials in light-emitting diodes. The substituted diphenyl-1,3,4-oxadiazoles are able to transport holes as well as electrons and show an intense fluorescence [19]. In our laboratory we have prepared poly(1,3,4-oxadiazole-imide)s, poly(1,3,4-oxadiazole-ester-imide)s and polyazomethines derived from an aromatic diamine 2-(4-dimethylaminophenyl)-5-(3,5-diaminophenyl)-1,3,4-oxadiazole [20-22]. Starting from another diamine, 4,4′-diamino-4″-[2-(4-phenoxy)-5-(4-dimethylaminophenyl)-1,3,4-oxadiazole]-triphenylmethane we prepared aromatic polyamides, polyimides, poly(amide-imide)s and polyazomethines having 2-(4-phenoxy)-5-(4-dimethylaminophenyl)-1,3,4-oxadiazole pendant groups [23-25]. These polymers showed fluorescence in solution and in solid state. Their solutions exhibited fluorescence in the blue region, with high quantum yield and large Stokes shift values. Protonation with HCl as a dopant caused a significant decrease of fluorescent intensity, due to the presence of nitrogen atoms with a free electron pair from 1,3,4-oxadiazole rings and dimethylamino groups.

Herein, as part of our continuing interest in the preparation of thermally stable polymers with special properties for different applications, we describe the synthesis of a new aromatic diamine, 2-(4,4′-diamino-4″-triphenylamine)-5-(4-dimethylaminophenyl)-1,3,4-oxadiazole, containing a triphenylamine unit, 1,3,4-oxadiazole ring and a dimethylamino group. Based on this diamine, a polyimide and three poly(amide-imide)s were prepared and characterized. The influence of the polymer structure on the properties, such as solubility, glass transition temperature, thermal stability and optical characteristics was studied. For one of the polymers a mechanism of thermal decomposition in nitrogen was proposed.

2. Experimental

1. Materials

4-Dimethylaminobenzohydrazide, 4-nitrobenzoyl chloride, 1-fluoro-4-nitrobenzene, 4,4′-(hexafluoroisopropylidene)diphthalic anhydride (**6FDA**), 4,4′-(4,4′-isopropylidenediphenyl-1,1′-diyldioxy)dianiline, phosphorus oxychloride ($POCl_3$), sodium hydrosulfide monohydrate, palladium on activated carbon (1 wt%) were provided from Aldrich and used as received. 1-Methyl-2-pyrrolidone (NMP) (Aldrich) was purified by stirring with NaOH and distilled from P_2O_5 prior to use. Pyridine (Aldrich) was purified by stirring with NaOH and distilled. Cesium fluoride (CsF) also purchased from Aldrich, was dried for 6 h at 160°C before use. The synthesis of 2,2-bis[*N*-(4-chloroformylphenyl)phthalimidyl]hexafluoropropane (**8**) and 2,2-bis[*N*-(4-chloroformylphenyl)phthalimidyl]dimethylsilane (**9**) was described elsewhere [26, 27].

2.2. Characterization

FTIR spectra were recorded on a Bruker Vertex 70 at frequencies ranging from 400 to 4000 cm^{-1} by using KBr pellets. The NMR spectra were recorded on a Bruker Avance III 400 spectrometer operating at 400.1 and 100.6 MHz for ^{1}H and ^{13}C nuclei respectively. Samples were recorded with either a 5 mm multinuclear inverse detection z-gradient probe (^{1}H spectra and all H-C 2D experiments) or with a 5 mm four nuclei direct detection z-gradient probe (^{13}C spectra). All the

experiments were recorded using standard pulse sequences, in the version with z-gradients for 2D spectra, as delivered by Bruker with TopSpin 2.1 PL6 spectrometer control and processing software. Chemical shifts are reported in δ units (ppm) and were referenced to the internal deuterated solvent for ^{1}H and ^{13}C chemical shifts (DMSO referenced at ^{1}H: 2.51 ppm and ^{13}C: 39.47 ppm). Electrospray ionization mass spectrometry (ESI-MS) was performed on an Agilent 6520 Series Accurate-Mass Q-TOF LC/MS. Data were collected and processed using MassHunter Workstation Software Data Acquisition for 6200/6500 Series, version B.01.03. The sample was dissolved in DMSO and diluted with methanol 1:9 (v/v), without added salt or acid prior to analysis. The molecular weights and their distribution were determined by gel permeation chromatography (GPC) with a PL-EMD 950 evaporative mass detector instrument. Two poly(styrene-co-divinylbenzene) gel columns (PLgel 5 μm Mixed-D and PLgel 5 μm Mixed-C) were used as stationary phase while *N*,*N*-dimethylformamide (DMF) was the mobile phase. The eluent flow rate was 1.0 mL min^{-1}. Polystyrene standards of known molecular weight were used for calibration. Differential Scanning Calorimetry (DSC) was performed on a Mettler Toledo DSC822^{e}. Approximately 10 mg of sample were tested applying a heating rate of 10ºC min^{-1} from 20 to 300ºC. Thermal stability was analyzed by means of a Mettler Toledo TGA-SDTA 851^{e} derivatograph. The thermogravimetric (TG) and derivative thermogravimetric (DTG) curves were recorded in nitrogen, with a flow of 20 mL min^{-1} in the temperature interval of 25-900°C and with the heating rate of 10°C min^{-1}. The coupled technique TG/MS/FTIR was applied using a device that is composed of a thermogravimetric analysis device types STA 449 F1 Jupiter (Netzsch, Germany), coupled with a spectrophotometer type Vertex-70 FTIR (Bruker, Germany) and a mass spectrometer QMS model 403 CAëolos (Netzsch, Germany). The analyzed sample mass ranged between 7.3 and 8.4 mg and the applied heating rate was 10°C min^{-1} in the temperature range of 25-680°C in nitrogen. Further information on the technical characteristics and operation of the TG/MS/FTIR system is detailed in a previous paper [28]. UV-visible absorption spectra were recorded in the 270-570 nm spectral range using an UV-visible spectrophotometer (Analytic Jena

210 Plus) and steady state fluorescence measurements were performed on a Perkin Elmer LS 55 fluorescence spectrometer. Fluorescence spectra were recorded between 350-670 nm, by exciting the polymer samples at the wavelength corresponding to the absorption maximum. The absolute fluorescence quantum yields were measured with an integrating sphere on an Edinburg Instruments FLS980 Spectrometer, at a concentration of 1.0×10^{-6} mol L^{-1}. Both the samples and reference were excited at the same wavelength. The Stokes shifts were calculated as the difference between the wavenumbers corresponding to the maxima of the absorption and emission bands. All the solvents of different polarities used for absorbance and fluorescence measurements were of spectrometric grade. All spectral measurements were performed at room temperature.

2.3. Synthesis

*2.3.1. N-(4-dimethylaminobenzoyl)-N'-(4-nitrobenzoyl)hydrazine (**3**)*

4-Dimethylaminobenzohydrazide (Aldrich) (4.475 g, 0.025 mol), NMP (35 mL) and pyridine (2 mL) were placed in a 100 mL three-necked flask equipped with mechanical stirrer, and the mixture was stirred until complete dissolution was achieved. The solution was cooled to 0°C, and 4-nitrobenzoyl chloride (4.637 g, 0.025 mol) was added under stirring. The flask content was kept at 0°C for 1 h and at room temperature for 6 h. The reaction mixture was poured in water while stirring, and the resulting precipitate was filtered, washed with water and dried. Yield: 85%. FTIR (KBr, cm^{-1}): 3252 (NH of hydrazide), 3020, 2918, 2865, 1680 (CONH), 1639 (CONH), 1605 and 1510 (-C-C- aromatic), 1372 (C-N), 1343 (NO_2). ^{1}H NMR ($CDCl_3$, 400 MHz) δ (ppm): 3.01 (6H, s, CH_3), 6.76 (2H, d, J = 8.8 Hz, H-3), 7.82 (2H, d, J = 8.8 Hz, H-2), 8.15 (2H, d, J = 8.8 Hz, H-2'), 8.38 (2H, d, J = 8.8 Hz, H-3'), 10.26 (1H, s, NH-6), 10.72 (1H, s, NH-6'). ^{13}C NMR ($CDCl_3$, 100 MHz) δ (ppm): 39.6 (2C, CH_3), 110.8 (2C, C-3), 118.6 (1C, C-1), 123.7 (2C, C-3'), 128.9 (4C, C-2 and C-2'), 138.4 (1C, C-1'), 149.3 (1C, C-4'), 152.5 (1C, C-4), 164.4 (1C, C-5'), 165.7 (1C, C-6). ESI-MS: calcd. for $C_{16}H_{16}N_4O_4$ m/z = 328.3226 [M^+], found m/z = 329.2577 [$M+H]^+$.

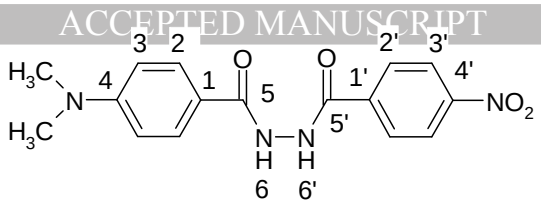

*2.3.2. 2-(4-Nitrophenyl)-5-(4′-dimethylaminophenyl)-1,3,4-oxadiazole (**4**)*

Compound **3** (4 g) and $POCl_3$ (50 mL) were introduced in a flask equipped with magnetic stirrer, and refluxed for 6 h. After cooling to room temperature, the reaction mixture was poured in an ice-water mixture, and the resulting precipitate was filtered, washed several times with water and dried. Yield: 87%. FTIR (KBr, cm^{-1}): 3025 (C-H aromatic), 2918 and 2865 ($N(CH_3)_2$), 1606 and 1510 (-C-C- aromatic), 1580 and 1341 (NO_2 stretching), 1017 and 960 (1,3,4-oxadiazole). ^{1}H NMR ($CDCl_3$, 400 MHz) δ (ppm): 2.88 (6H, s, CH_3), 6.56 (2H, d, J = 8.8 Hz, H-3”), 7.76 (2H, d, J = 9.2 Hz, H-2”), 8.09 (2H, d, J = 8.8 Hz, H-2’), 8.17 (2H, d, J = 8.8 Hz, H-3’). ^{13}C NMR ($CDCl_3$, 100 MHz) δ (ppm): 39.5 (2C, CH_3), 109.22 (1C, C-1”), 111.1 (2C, C-3”), 123.8 (2C, C-3’), 126.9 (2C, C-2’), 128.0 (2C, C-2”), 129.3 (1C, C-1’), 148.6 (1C, C-4’), 152.2 (1C, C-4”), 161.2 (1C, C-2), 165.8 (1C, C-5). ESI-MS: calcd. for $C_{16}H_{14}N_4O_3$ m/z = 310.3074 [M^+], found m/z = 311.2457 $[M+H]^+$.

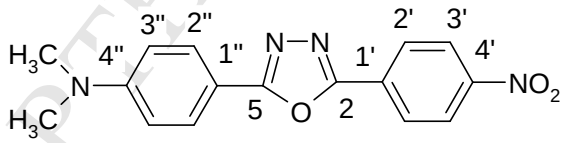

*2.3.3. 2-(4-Aminophenyl)-5-(4′-dimethylaminophenyl)-1,3,4-oxadiazole (**5**)*

Compound **4** (8 g, 0.0334 mol) was dissolved in 250 mL boiling ethanol. To this boiling solution sodium hydrosulfide monohydrate (10 g) was added within 20 min and after a half hour a clear dark green solution was obtained. The hot ethanol solution was filtered and after cooling to room temperature a white precipitate was separated. Yield: 82%. FTIR (KBr, cm^{-1}): 3447, 3350 and 3220 (NH_2), 3037 (aromatic C-H), 2915 and 2853 ($N(CH_3)_2$), 1608, 1495 (C-C aromatic), 1011 and 960 (1,3,4-oxadiazole). ^{1}H NMR ($CDCl_3$, 400 MHz) δ (ppm): 3.05 (6H, s, CH_3), 4.03 (2H, bs, NH_2), 6.75 (4H, d, J = 8.8 Hz, H-3’ and H-3”), 7.90 (2H, d, J = 8.4 Hz, H-2’), 7.95 (2H, d, J = 8.8 Hz, H-2”). ^{13}C NMR ($CDCl_3$, 100 MHz) δ (ppm): 40.1 (2C, CH_3), 111.4 (1C, C-1”), 111.6 (2C, C-

3"), 114.2 (1C, C-1'), 114.7 (2C, C-3'), 128.1 (2C, C-2"), 128.4 (2C, C-2'), 149.3 (1C, C-4'), 152.1 (1C, C-4"), 163.9 (1C, C-2), 164.4 (1C, C-5). ESI-MS: calcd. for $C_{16}H_{16}N_4O$ m/z = 280.3244 [M^+], found m/z = 281.2570 [M+H]$^+$.

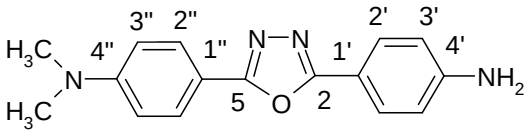

*2.3.4. 2-(4,4'-Dinitro-4″-triphenylamine)-5-(4-dimethylaminophenyl)-1,3,4-oxadiazole (**6**)*

Compound **5** (5.54 g, 19.79 mmol), CsF (10.52 g, 69.29 mmol), 1-fluoro-4-nitrobenzene (5.6 g, 20 mmol) and DMSO (70 mL) were added in a three necked flask. The reaction mixture was heated at 140°C under stirring and inert atmosphere for 24 h, it was cooled to room temperature and precipitated into water. The yellow precipitate was then collected by filtration and washed with water. Yield: 69%. Mp. 235-237°C. FTIR (KBr, cm^{-1}): 3079 (aromatic C-H stretching), 2910 and 2869 (aliphatic C-H stretching), 1600 and 1504 (aromatic C-C stretching), 1580 and 1341 (NO_2 stretching), 1008 and 954 (oxadiazole ring), 845 (C-N stretching for aromatic NO_2). ^{1}H NMR ($CDCl_3$, 400 MHz) δ (ppm): 3.07 (6H, s, CH_3), 6.76 (2H, d, J = 8.8 Hz, H-3"), 7.22 (4H, d, J = 9.2 Hz, H-3*), 7.28 (2H, d, J = 8.8 Hz, H-3'), 7.97 (2H, d, J = 8.8 Hz, H-2"), 8.13 (2H, d, J = 8.4 Hz, H-2'), 8.19 (4H, d, J = 9.2 Hz, H-2*). ^{13}C NMR ($CDCl_3$, 100 MHz) δ (ppm): 40.1 (2C, CH_3), 110.5 (1C, C-1"), 111.6 (2C, C-3"), 122.2 (1C. C-1'), 123.3 (4C, C-3*), 125.7 (4C, C-2*), 126.4 (2C, C-3'), 128.4 (2C, C-2"), 128.7 (2C, C-2'), 143.4 (2C, C-1*), 147.4 (1C, C-4'), 151.3 (2C, C-4*), 152.5 (1C, C-4"), 162.5 (1C, C-2), 165.5 (1C, C-5). ESI-MS: calcd. for $C_{28}H_{22}N_6O_5$ m/z = 522.5115 [M^+], found m/z = 523.2763 [M+H]$^+$.

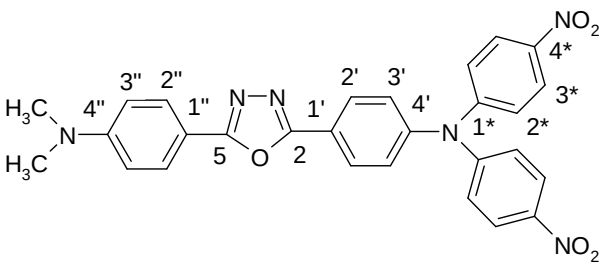

*2.3.5. 2-(4,4′-diamino-4″-triphenylamine)-5-(4-dimethylaminophenyl)-1,3,4-oxadiazole (**7**)*

The dinitro compound **6** (9 g, 15.10 mmol), Pd/C (Pd content 1%, 0.46 g), and ethanol (200 mL) were introduced in a three neck round-bottom flask. Hydrazine monohydrate (70 mL) was slowly added and the reaction mixture was heated to reflux for 12 h. The hot mixture was filtered to remove Pd/C and the solvent was evaporated. The resulting product was recrystallized from ethanol. Yield 26%. Mp. = 248-249°C. FTIR (KBr, cm^{-1}): 3456, 3350, 3220 (NH_2), 3028 (C-H aromatic), 2907, 2857 (C–H aliphatic), 1610, 1500 (aromatic C-C stretching), 1010, 950 (oxadiazole ring). ^{1}H NMR ($CDCl_3$, 400 MHz) δ (ppm): 3.05 (6H, s, CH_3), 5.12 (4H, bs, NH_2), 6.66 (4H, d, *J* = 8.6 Hz, H-3*), 6.75 (2H, d, *J* = 9.0 Hz, H-3”), 6.89 (2H, d, *J* = 8.8 Hz, H-3’), 7.00 (4H, d, *J* = 8.6 Hz, H-2*), 7.82 (2H, d, *J* = 8.8 Hz, H-2’), 7.94 (2H, d, *J* = 8.8 Hz, H-2”). ^{13}C NMR ($CDCl_3$, 100 MHz) δ (ppm): 40.1 (2C, CH_3), 111.5 (1C, C-1”), 111.6 (2C, C-3”), 114 (1C, C-1’), 116.1 (4C, C-3*), 117.5 (2C, C-3’), 127.6 (2C, C-2’), 127.7 (4C, C-2*), 128.1 (2C, C-2”), 137.9 (2C, C-1*), 143.5 (2C, C-4*), 151.6 (1C, C-4’), 152.1 (1C, C-4”), 163.9 (1C, C-2), 164.3 (1C, C-5). UV-Vis (DMSO): = 364 nm. Fluorescence (DMSO): λ_{em} = 412 nm, SS = 48 nm, QY = 8.28%. ESI-MS: calcd. for $C_{28}H_{26}N_6O$ m/z = 462.5458 [M^+], found m/z = 463.3731 [M+H]$^+$.

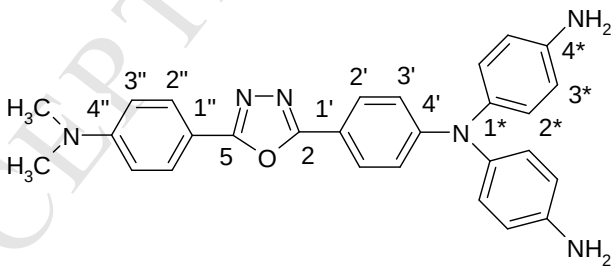

*2.3.6. Synthesis of poly(amide-imide)s **10a**, **10b** and **10c***

The poly(amide-imide)s **10a-c** were synthesized by solution polycondensation reaction of diamine **7** with diacid chlorides **8** or **9**, in NMP as a solvent and in the presence of pyridine as acid acceptor. In a typical experiment, **10a** was prepared as follows: diamine **7** (0.462 g, 0.001 mol), NMP (6 mL) and pyridine (0.2 mL) were introduced into a flask and the mixture was stirred under nitrogen until complete dissolution. Diacid chloride **8** (0.719 g, 0.001 mol) was added and the

reaction mixture was stirred for 10 h to yield a viscous polymer solution. The solution was diluted to about 5% by addition of more NMP and the polymer was precipitated by pouring into methanol. The precipitated product was filtered, washed with ethanol and water and dried under vacuum at 110°C for 10 h to give poly(amide-imide) **10a**. The poly(amide-imide) **10b** was prepared starting from **7** (0.462 g, 0.001 mol) and diacid chloride **9** (0.627 g, 0.001 mol) while copolyamide **10c** was prepared from diacid chloride **8** (0.719, 0.001 mol) and a mixture of **8** (0.231 g, 0.0005 mol) and 4,4′-(4,4′-isopropylidenediphenyl-1,1′-diyldioxy)dianiline (0.205 g, 0.0005 mol).

10a

FTIR (KBr, cm^{-1}): 3430 (NH stretching), 3043 (aromatic C-H), 2922, 2855 (C-H aliphatic), 1786 and 1726 (C=O of imide ring), 1671 (C=O of amide) 1610 and 1508 (C-C aromatic) 1368 (C-N of imide ring), 1192 and 1210 (C-F), 1017 and 961 (1,3,4-oxadiazole ring), 720 (C=O bending of imide ring). ^{1}H NMR (DMSO-d6, 400 MHz) δ (ppm): 3.02 (6H, s, CH_3), 6.85 (2H, bs, H-2), 7.02 (2H, bs, H-9), 7.20 (4H, bs, H-12), 7.64 (4H, d, J = 7.2 Hz, H-18), 7.79 (2H, bs, H-23), 7.85 (6H, bs, H-3 and H-13), 7.91 (2H, bs, H-8), 8.00 (2H, bs, H-25), 8.10 (4H, d, J = 8.4 Hz, H-17), 8.22 (2H, bs, H-26), 10.45 (2H, bs, NH). ^{13}C NMR (DMSO-d6, 100 MHz) δ (ppm): 39.7 (2C, CH_3), 64.6 (1C, heptet, $J_{C,F}$ = 25 Hz, C-28), 109.9 (1C, C-4), 111.7 (2C, C-2), 114.9 (1C, C-7), 119.3 (2C, C-9), 121.7 (4C, C-13), 123.3 (2C, q, $J_{C,F}$ = 287 Hz, C-29), 123.7 (2C, C-23), 124.5 (2C, C-26), 126.1 (4C, C-12), 127.1 (4C, C-18), 127.7 (4C, C-3 and C-8), 128.3 (4C, C-17), 132.6 (2C, C-22), 132.9 (2C, C-27), 134.4 (2C, C-19), 134.7 (2C, C-16), 135.9 (4C, C-14 and C-25), 137.4 (2C, C-24), 141.6 (2C, C-11), 150.3 (1C, C-10), 152.2 (1C, C-1), 162.8 (1C, C-6), 163.9 (1C, C-5), 164.9 (2C, C-15), 165.7 and 165.9 (4C, C-20 and C-21). UV-Vis (DMSO): λ_{abs} = 372 nm. Fluorescence (DMSO): λ_{em} = 469 nm, SS = 92 nm, QY = 0.11%. GPC: M_n = 19500 g mol^{-1}, M_w =25700 g mol^{-1}, PDI = 1.32.

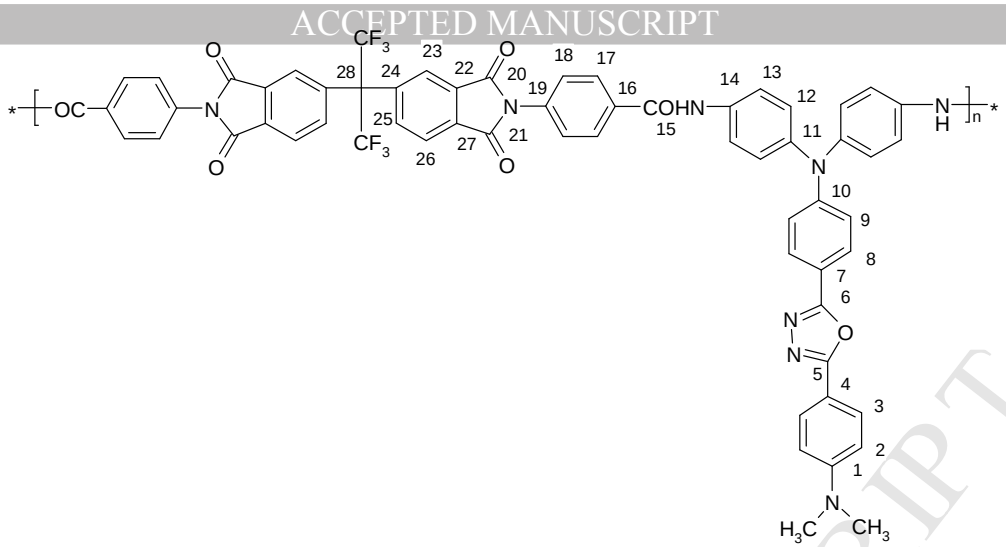

10b

FTIR (KBr, cm^{-1}): 3384 (N-H stretching), 3043 (aromatic C-H), 2923, 2854 (C-H aliphatic), 1786 and 1726 (C=O of imide ring), 1671 (C=O of amide), 1608 and 1504 (C-H aromatic), 1368 (C-N of imide ring), 1017 and 965 (1,3,4-oxadiazole ring), 1260 and 810 (Si-C stretching), 719 (C=O bending of imide ring). ^{1}H NMR (DMSO-d6, 400 MHz) δ (ppm): 0.80 (6H, bs, CH_3-Si), 3.02 (6H, s, CH_3), 6.85 (2H, bs, H-2), 7.02 (2H, bs, H-9), 7.20 (4H, bs, H-12), 7.63 (4H, d, J = 8.1 Hz, H-18), 7.85 (6H, bs, H-3 and H-13), 7.90 (2H, bs, H-8), 8.01 (2H, bs, H-26), 8.09 (4H, d, J = 8.3 Hz, H-17), 8.12-8.15 (4H, m, H-23 and H-25), 10.42 (2H, bs, NH). ^{13}C NMR (DMSO-d6, 100 MHz) δ (ppm): -3.3 (2C, CH_3-Si), 39.7 (2C, CH_3), 109.9 (1C, C-4), 111.7 (2C, C-2), 115.0 (1C, C-7), 119.3 (2C, C-9), 121.6 (4C, C-13), 122.7 (2C, C-26), 125.4 (4C, C-12), 127.0 (4C, C-18), 127.7 (4C, C-3 and C-8), 128.2 (4C, C-17), 128.4 (2C, C-23), 130.8 (2C, C-22), 132.5 (2C, C-27), 134.3 (2C, C-16), 134.6 (2C, C-19), 135.9 (2C, C-14), 140.3 (2C, C-25), 141.5 (2C, C-11), 145.7 (2C, C-24), 150.3 (1C, C-10), 152.1 (1C, C-1), 162.8 (1C, C-6), 163.9 (1C, C-5), 164.8 (2C, C-15), 166.6 and 166.9 (4C, C-20 and C-21). UV-Vis (DMSO): λ_{abs} = 373 nm. Fluorescence (DMSO): λ_{em}= 423 nm, SS = 50 nm, QY = 0.88%. GPC: M_n = 33600 g mol^{-1}, M_w = 46100 g mol^{-1}, PDI = 1.37.

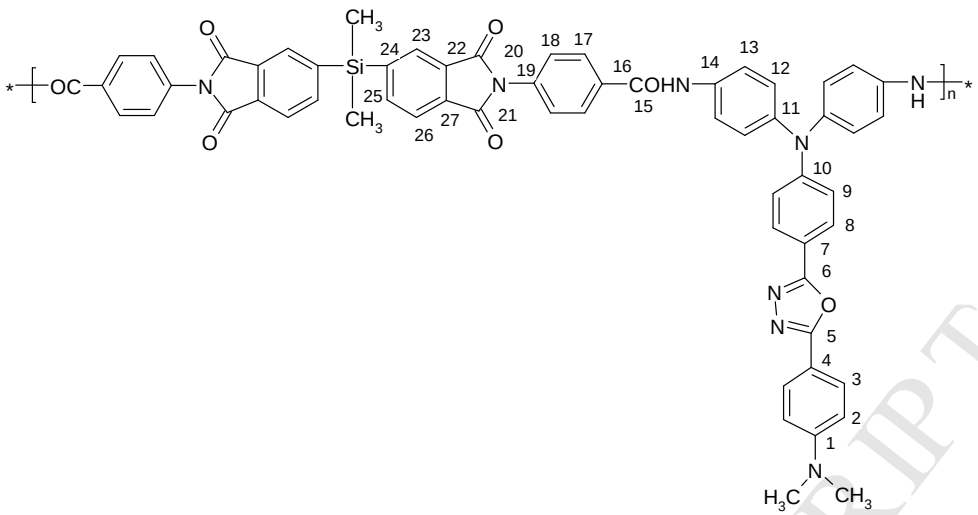

10c

FTIR (KBr, cm^{-1}): 3429 (N-H stretching), 3041 (C-H aromatic), 2953, 2921, 2853 (C-H aliphatic), 1777, 1721 (C=O of imide ring), 1669 (C=O of amide), 1609 and 1507 (C-H aromatic), 1364 (C-N of imide ring), 1220 (aromatic -C-O-C-), 1209 and 1190 (C-F), 1017 and 955 (1,3,4-oxadiazole ring). ^{1}H NMR (DMSO-d6, 400 MHz) δ (ppm): 3.02 (6H, s, CH_3), 6.62 (s), 6.71 (d, J = 7.8 Hz), 6.85 (2H, d, J = 8.1 Hz), 7.04 (2H, d, J = 8.5 Hz), 7.11 (d, J = 8.4 Hz), 7.22 (4H, d, J = 7.8 Hz), 7.36 (t, J = 7.7 Hz), 7.64 (4H, d, J = 7.0 Hz), 7.79 (2H, bs), 7.83-7.85 (6H, m), 7.93 (2H, d, J = 8.4 Hz), 8.00 (2H, bs), 8.10 (4H, d, J = 7.6 Hz), 8.22 (2H, d, J = 5.6 Hz), 10.41 (2H, bs, NH). 10.45 (2H, bs, NH). ^{13}C NMR (DMSO-d6, 100 MHz) δ (ppm): 39.7 (2C, CH_3), 64.6 (1C, heptet, $J_{C,F}$ = 25 Hz), 107.4 (CH), 109.9 (1C), 111.7 (2C), 112.0 (CH), 115.0 (1C), 119.3 (2C), 119.6 (CH), 121.6 (4C), 121.9 (CH), 123.3 (2C, q, $J_{C,F}$ = 287 Hz), 123.7 (2C), 124.4 (2C), 126.0 (4C), 127.0 (4C), 127.6 (4C), 128.2 (4C), 130.9 (CH), 132.5 (2C), 132.9 (2C), 134.3 (2C), 134.6 (2C), 135.2 (C), 135.8 (4C), 137.4 (2C), 141.6 (2C), 150.3 (1C), 151.6 (C), 152.1 (1C), 158.7 (C), 162.8 (1C), 163.9 (1C), 164.8 (2C), 165.7 and 165.9 (4C). UV-Vis (DMSO): λ_{abs} = 373 nm. Fluorescence (DMSO): λ_{em} = 452 nm, SS = 79 nm, QY = 0.18%. GPC: **10c**: M_n = 28800 g mol^{-1}, M_w= 36100 g mol^{-1}, PDI = 1.25.

*2.3.7. Synthesis of polyimide **11***

Polyimide **11** was prepared by a two-step polycondensation reaction of diamine **7** with dianhydride **6FDA.** In a 100 mL three-necked flask equipped with mechanical stirrer and nitrogen-inlet and outlet were introduced diamine **7** (0.462 g, 0.001 mol) and NMP (6 mL). The mixture was stirred under nitrogen to the complete dissolution and **6FDA** (0.444 g, 0.007 mol) was added and stirring was continued for 12 h. Then, pyridine (3 mL) and acetic anhydride (2 mL) were added and the resulting solution was heated at 100°C for 4 h. The flask was cooled-down to room temperature and the solution was poured into methanol to precipitate the polymer. The solid product was filtered, washed three times with water under stirring and dried at 100°C. FTIR (KBr, cm^{-1}): 3070 (C-H aromatic), 2931, 2850 (C-H aliphatic), 1784 and 1725 (C=O of imide ring), 1612 and 1500 (-C-C- aromatic), 1210 and 1192 (C-F), 720 (C=O bending of imide ring). ^{1}H NMR (DMSO-d6, 400 MHz) δ (ppm): 3.02 (6H, s, CH_3), 6.85 (2H, bs, H-2), 7.21 (2H, bs, H-9), 7.32 (4H, bs, H-12), 7.48 (4H, bs, H-13), 7.78 (2H, bs, H-18), 7.86 (2H, bs, H-3), 7.96-8.01 (4H, m, H-3 and H-20), 8.20 (2H, bs, H-21). ^{13}C NMR (DMSO-d6, 100 MHz) δ (ppm): 39.7 (2C, CH_3), 64.5 (1C, heptet, $J_{C,F}$ = 25 Hz, C-28), 109.8 (1C, C-4), 111.7 (2C, C-2), 117.2 (1C, C-7), 122.3 (2C, C-9), 123.3 (2C, q, $J_{C,F}$ = 291 Hz, C-29), 123.5 (4C, C-18), 124.3 (2C, C-21), 125.1 (4C, C-12), 127.5 (4C, C-14), 127.7 (2C, C-3), 127.9 (2C, C-8), 128.7 (4C, C-13), 132.6 (2C, C-17), 132.9 (2C, C-22), 135.8 (2C, C-20), 137.5 (2C, C-19), 145.7 (2C, C-11), 149.5 (1C, C-10), 152.2 (1C, C-1), 162.6 (1C, C-6), 164.2 (1C, C-5), 165.9 and 166.0 (4C, C-15 and C-16). UV-Vis (DMSO): λ_{abs} = 369 nm. Fluorescence (DMSO): λ_{em} = 417 nm, SS = 43 nm, QY = 1.30%. GPC: **11**: M_n = 9200 g mol^{-1}, M_w = 12400 g mol^{-1}, PDI = 1.35.

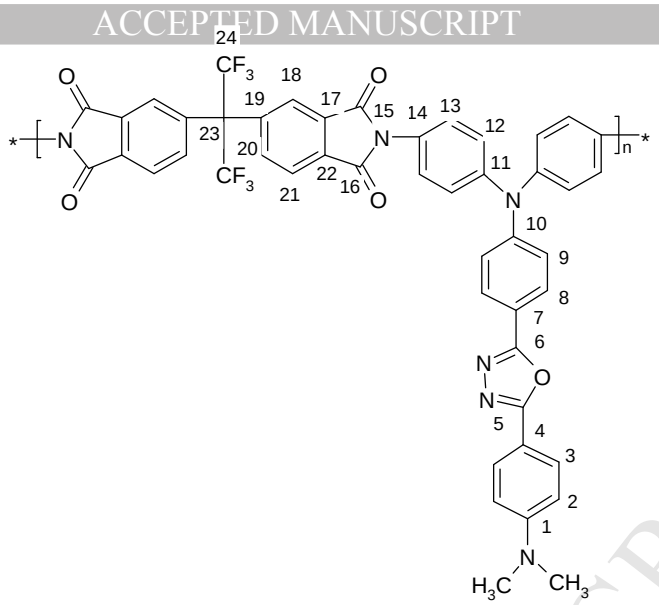

3. Results and discussion

*3.1. Synthesis of diamine **7***

A new diamine **7** was prepared through a sequence of reactions, as shown in scheme 1. Dimethylaminobenzohydrazide reacted with 4-nitrobenzoyl chloride in NMP as solvent and pyridine as catalyst, resulting in compound **3** containing a nitro group. This compound was treated with $POCl_3$ to give the corresponding oxadiazole nitro derivate **4**. The reduction of **4** with sodium hydrosulfite in ethanol afforded the amino oxadiazole derivative **5**. Compound **6** was prepared starting from **5** and 1-fluoro-4-nitrobenzene in the presence of CsF. The hydrogenation of **6** was further performed by using hydrazine hydrate and a catalytic amount of Pd/C to obtain the diamine **7**. The structure of the compounds **3-7** was confirmed by FTIR and NMR spectroscopy. Unambiguous assignments for the ^{1}H and ^{13}C chemical shifts were based on two-dimensional homo- and heteronuclear correlations like $^{1}H,^{1}H$-COSY (Correlation Spectroscopy), $^{1}H,^{13}C$ HSQC (Heteronuclear Single Quantum Coherence) as well as HMBC (Heteronuclear Multiple Bond Coherence). All the spectra were in good agreement with the proposed structures. In the FTIR spectrum of **7** characteristic absorption bands appeared at 3456, 3350 and 3220 (NH asymmetric and symmetric stretching), 2954 and 2857 (C-H aliphatic), and at 1013 and 944 cm^{-1} (=C-O-C=

stretching in oxadiazole ring) confirming the presence of primary amine and dimethylamine groups, and 1,3,4-oxadiazole ring (Fig. S1 of the Supplementary material). Fig. 1 represents the ^{1}H NMR spectrum of **7** with the assignment for all the protons. The protons in *ortho* position to the amine groups appeared at 6.66 ppm as a doublet while the protons in *ortho* position to oxadiazole ring appeared as doublet at the highest ppm values. The protons of aromatic amine groups appeared as a singlet at 5.12 ppm.

Scheme 1

Figure 1

3.2. Synthesis and general characterization of the polymers

The poly(amide-imide)s **10a** and **10b** were prepared by low-temperature solution polycondensation reaction of **7** with two diacid chlorides containing imide rings **8** and **9**, respectively. The copolyimide **10c** was synthesized starting from the diacid chloride **8** and an equimolar mixture of diamines **7** and 4,4′-(4,4′-isopropylidenediphenyl-1,1′-diyldioxy)dianiline. The polyimide **11** was obtained in two steps; in the first step a polyamic acid was prepared by polycondensation reaction of an equimolar amount of **7** and **6FDA**, in NMP as solvent. In the second step the poly(amic acid) was chemically cyclized in the presence of acetic anhydride and pyridine. The chemical structure of the polymers is illustrated in Fig. 2.

Figure 2

The structure of the polymers was confirmed by FTIR and ^{1}H NMR. In the FTIR spectra of all the polymers characteristic absorption bands appeared at around 1780, 1720, 1360 and 720 (imide ring), at 1015 and 950 (1,3,4-oxadiazole ring) and at 2919 and 2855 cm^{-1} (aliphatic C-H groups) (Fig. S2 of the Supplementary material). FTIR spectra of **10a**, **10c** and **11** showed characteristic absorption bands for 6F groups at around 1180 and 1210 cm^{-1} (C-F stretching). The FTIR spectrum of **10b** presented a specific absorption band at 810 cm^{-1} (Si-C stretching). The ^{1}H NMR spectra of **10a**, **10b** and **10c** showed characteristic peaks of amide groups at about 10.4 ppm (see Fig. 3 for **10a**).

Figure 3

All the polymers were easily soluble in polar organic solvents such as NMP, DMF, N,N-dimethylacetamide (DMAc) and DMSO. The polyimide **11** was soluble in chloroform and tetrahydrofuran while the poly(amide-imide)s were insoluble in these solvents. The good solubility can be explained by the presence of 6F or dimethylsilane groups in their chemical structure, which increased the flexibility of the macromolecular chains thus enhancing the solubility. The molecular weight was determined by GPC. The number average molecular weight (M_n) values of **10a**, **10b**, **10c** and **11** were of 19500, 33600, 28800, 9200 g mol^{-1}, respectively, the weight average molecular weight (M_w) values were of 25700, 46100, 36100, 12400 g mol^{-1}, respectively, and the polydispersity index (PDI) was of 1.32,1.37, 1.25, 1.35, respectively.

3.3. Influence of the structure on the thermal stability

The thermal behavior of the polymers was investigated by DSC and TGA. The DSC measurements did not evidence a glass transition temperature in the measurement domain. This can be explained by a high rigidity of macromolecular chains due to the presence of 2-(4-phenoxy)-5-(4-dimethylaminophenyl)-1,3,4-oxadiazole pendant groups which may produce steric hindrance. The main thermogravimetric characteristics obtained from the analysis of the TG and DTG curves are presented in Table 1. The DTG curves are comparatively shown in Fig. 4. The obtained results reveal that polymer degradation comprised two or three stages. A significant amount of residue resulted at 900°C, which is the temperature at which the heating process ended. If the thermal decomposition onset temperature is taken as the thermal stability criterion, the series of thermal stability increase is: **10b<11<10c≅10a.**

Figure 4

Table 1

The analysis of the results shows the same thermal stability for **10a** and **10c**, as well as approximately the same thermal decomposition onset temperature and approximately the same T_{Peak} in the first stage. In their cases, the thermal decomposition initiation probably occurred in the same

groups which exist in both structures. A prior study [29], which applied the TG/MS/FTIR technique to other polymers containing oxadiazole in their side chain, established that thermal decomposition initiation occurs in the methyl groups and the oxadiazole in the side chain. The thermal decomposition in inert atmosphere of **11** included three stages, where the second T_{Peak} had approximately the same value as **10a** polymer and **10c** copolymer. A different behavior of **10b** was found, which exhibits the lowest thermal stability when the thermal decomposition onset temperature is considered as the thermal stability criterion. The temperature peak of approximately 544°C was not detected for this polymer. In order to clarify aspects related to the thermal degradation mechanism of this polymer, the coupled TG/MS/FTIR technique in inert atmosphere (nitrogen) was used. The obtained MS spectra revealed that thermal decomposition initiation is probably due to the *a* and *b* scissions in the side chains, and to the *c* scission in the amidic group (see scheme 2). This assumption is supported by the presence of ionic fragments m/z=15 (CH_3^+), m/z = 93 ($C_6H_5NH_2^+$) and m/z = 103 ($C_6H_5CN^+$) (see Fig. 5a and 5b). At temperatures higher than 540°C, the decomposition continued with the *d* scissions in the imide group (see scheme 2). Special mention should be made of the ionic fragment m/z = 103 the intensity of which increased and reached a temperature peak of approximately 580°C. It may be associated with benzonitrile ($C_6H_5CN^+$) which may result, together with the ionic fragment m/z = 44 (CO_2^+) and the fragment m/z = 28 (CO^+), from the imide group degradation (see Fig. S3 of the Supplementary material). The ionic fragments m/z = 78 (C_6H_6) and m/z = 30 (CH_2O^+) was also identified in the MS spectra at temperatures higher than 540°C (see Fig. 5c and 5d). Fig. S4 of the Supplementary material also shows ionic current variation with temperature increase for other ionic fragments, on which we relied when we suggested the degradation mechanism described in scheme 2, like for instance: m/z = 18 (H_2O^+), and also m/z = 58 ($Si(CH_3)_2$) and m/z = 128 ($NCC_6H_4CN^+$), with lower intensity for ionic current.

The degradation mechanism suggested for **10b** is also supported by the FTIR analysis of the solid residue resulting after sample heating in nitrogen at a rate of 10°C min^{-1} up to 540 and up to

650°C. The structure of **10b** was identified by FTIR spectroscopy (Fig. S5 of the Supplementary material). In the FTIR spectra of **10b** characteristic absorption bands for imide rings appeared at 1786, 1726, 1360 and 732 cm^{-1} (imide rings), 1671 (amide groups), 1017 and 965 (oxadiazole ring) and 1260 and 810 cm^{-1} (Si-CH_3). In the case of the same polymer heated up to 540°C with the heating rate of 10°C min^{-1} it can be observed a significant decrease of the absorption band at 1671 cm^{-1}, due to the partial decomposition of amide groups, and the disappearance of the absorption bands of 1017 and 965 cm^{-1}, due to the decomposition of oxadiazole rings. A strong absorption band appeared at 2220 cm^{-1} probably due to the formation of CN groups. In the FTIR spectrum of the polymer heated up to 640°C the absorption bands characteristic for the imide rings at 1786, 1726, 1360 and 732 cm^{-1} were not observed. Characteristic bands can be seen at 1620 (aromatic systems), and at 1080 cm^{-1} (very broad) due to the formation of Si-O-Si groups.

Scheme 2

Figure 5

Fig. 6 shows a comparison between the FTIR spectra obtained by the coupled TG/FTIR technique for different temperatures, with a view to determining the degradation mechanism of **10b**. It can be concluded that the results were in agreement with the previous results of the MS spectra analysis. Water-specific bands ranged between 4000 and 3400 cm^{-1}, CO_2-specific bands ranged between 2400 and 2200 cm^{-1} and between 740 and 600 cm^{-1}, and benzene-specific bands ranged between 1600 and 1400 cm^{-1} [30]. An intense peak at approximately 3015 cm^{-1} was identified, which agrees with the literature data [31] and may be associated with the presence of CH_4. Intensity peak at 1373 cm^{-1} indicates the presence of benzonitrile [32], whereas the 2180 and 2108 cm^{-1} peaks may be associated with the presence of carbon monoxide [33], results which were also supported by the MS spectra shown in Fig S3 in the Supplementary material, for the ionic fragment m/z = 28 (CO^+). A 1265 cm^{-1} peak specific to amines [34] and a 1730 cm^{-1} peak specific to carbonyl compounds [35] were also identified, thus confirming the presence of ionic fragments m/z = 93 ($C_6H_5NH_2^+$) and m/z = 30 (CH_2O^+).

Figure 6

3.4. Optical properties

The optical properties of the new polymers were investigated by absorption and fluorescence spectra in different solvents, namely NMP (ε = 33.0), DMF (ε = 38.25), DMAc (ε = 37.8) and DMSO (ε = 46.7). The absorption and fluorescence data were collected in Table 2. In all selected solvents these compounds exhibited a strong absorption band located in the range of 357-373 nm, attributed to the π-π* transitions resulting from the conjugation between the aromatic rings and nitrogen atoms (see Fig. 7a). The absorption spectra of **10a** with amide groups in the backbone exhibited red shifts in all solvents (NMP (18 nm), DMF (19 nm), DMAc (10 nm) and DMSO (20 nm)) in comparison with that of corresponding polyimide **11** (see Table 2). These red shifts of the absorption maxima are due to the specific solute-solvent interactions and indicate longer conjugation.

On the other hand, the absorption spectra for all samples were slightly affected by changes in the physical properties of the solvating media (the bathochromic shift caused by solvent was only cca. 10 nm, as can be seen in Fig. 7, for compound **10a**).

Figure 7

Table 2

Fig. 8 shows the fluorescence spectra of the investigated samples in various solvents. These spectra exhibit a single emission band in all solvents, with the emission maximum centered between 407 and 473 nm in the blue region (see Fig. 8a). The emission maximum presents anomalous blue shifts (39 and 46 nm) in DMF and DMSO solutions, respectively from **10a** to **10b** (see Table 2 and Fig. 8b), due to the presence of a flexible dimethylsilane bridge that introduces a deviation from the linearity of the chains. The copolymer **10c** had an emission maximum around 451 nm that is blue shifted in DMF and DMSO solutions in comparison with that of the corresponding poly(amide-imide) **10a**. Moreover**,** the hypsochromic shifts (24 nm and 13 nm) in emission maxima of **10a** were observed in DMF and DMSO compared to NMP and DMAc solvents, while for **10b** some

bathochromic shifts (17 and 33 nm) were found in DMF and DMSO compared to that of NMP and DMAc solutions. These shifts in the fluorescence maxima are a consequence of the specific solute-solvent interactions from the system (the reorganization of local environments due to hydrogen bonding formation). Also, the positive solvatochromic behavior of **10b** in DMF and DMSO solutions indicates greater stabilization of the excited singlet state of the compound in these solvents compared to NMP and DMAc solvents**,** while the absorption spectra are slightly affected by solvent characteristics. In all studied solvents, **10a, 10b** and **10c** have the most red-shifted emission maximum, like in absorption, compared to those of the corresponding diamine **7** and polyimide **11**, that can be due to the its longer conjugation length and to electro-affinities of 6F units which influence the π-π^* transitions (see Table 2). Also, the fluorescence bands (full width at half-maximum of the fluorescence band, $FWHM_{em}$) for **10a, 10b** and **10c** in all selected solvents (see Table 2) are larger than that of the corresponding diamine **7** or polyimide **11**, indicating that the conjugation length is more precisely controlled (shorter conjugation) in diamine **7** and polyimide **11** [35] and the solvents influenced easily the spectral properties of these samples. For these newly developed polyimide and poly(amide-imde)s the Commission Internationale de L'Eclairage ($CIE_{x,y}$) coordinates were evaluated to be (**7:** 0.15, 0.06; **10a:** 0.18, 0.10; **10b:** 0.16, 0.04; **10c:** 0.19, 0.10; and **11:** 0.18, 0.12) indicating blue emission.

Figure 8

For all investigated compounds, the large values of Stokes shifts (40-100 nm, see Table 2) in each of the solvents at room temperature were estimated. The polymer **10a** has larger Stokes shifts values in DMF and DMSO solutions due to considerable media (solvent) reorganization originated from the hydrogen bonding formation [36].

The fluorescence quantum yields (QY, %) of the polymers in dilute DMSO solution are listed in Table 2. The highest QY value of 8.28 % was observed for diamine **7**, that is much higher than that of corresponding polyimides and poly(amide-imide)s. The polymers **10a** and **10c** had the

lowest QY values of around 0.1 %. The luminescence quantum yields range from 0.11 to 8.28%, thereby indicating a quenching effect for the compounds derived from diamine **7**.

Figs. 9a and 9b display the emission spectra of poly(amide-imide) **10b** and diamine **7** with an increase of excitation wavelength from 363 to 415 nm. Fluorescence spectra displayed an emission pattern slightly dependent on the excitation wavelength (Fig. 9a), namely it can be found that as the excitation wavelength increased the emission band decreased in intensity and a shift to longer wavelengths (a very small red shift) appeared. These small red shifts can be associated with a strong correspondence between excitation energy and the vibronic structure of the emission spectra [37] and with the existence of many binding species in the system, due to the more intense interactions between solute and solvent [38]. Also, from Fig. 9a was observed that for **10b** the spectral shifts are followed by a slightly decrease in fluorescence band width (the full width at half-maximum of the emission band, $FWHM_{em}$), while for corresponding diamine **7** and polyimide **11** no changes in the position and shape of the emission band were recorded as the excitation wavelength increased (Fig. 9b). Similar behavior was observed in all investigated compounds in selected solvents. Compared to **10a, 10b** and **10c**, the emission spectra of diamine **7** and polyimide **11** are less sensitive to the excitation wavelength values.

Figure 9

The studied polymers have different numbers of nitrogen atoms which can be susceptible to protonation. Thus, the influence of dilute HCl solution on the absorption and fluorescence spectra of **10a** in NMP solution was monitored. The changes observed in the UV-Vis spectra of **10a** in NMP solution were shown in Fig. 10a. The increase in the concentration of HCl led to the progressive enhancement of the absorption intensities from 313 and 386 nm, respectively. These changes in absorption intensities indicate the presence of more than one protonated species in solution [39]**.** Fig. **10b** shows the fluorescence response of **10a** in acidic medium where a gradual decreases in emission intensity and small blue shift (the emission maximum of the solution containing 650 μL HCl was moved to 435 nm with respect to neutral solution) of emission band

with a progressive increase in acid strength of the medium were observed. These changes in emission spectral characteristics are attributed to a protonation process of the nitrogen atoms.

Figure 10

4. Conclusions

A new aromatic diamine 2-(4,4′-diamino-4″-triphenylamine)-5-(4-dimethylaminophenyl)-1,3,4-oxadiazole was synthesized and used for the preparation of a polyimide and three poly(amide imide)s. The polymers were soluble in organic solvents and exhibited high thermal stability, with decomposition temperature above 380°C. A mechanism of thermal decomposition in nitrogen of a poly(amide-imide) was estimated by using the coupled TG/MS/FTIR techniques. The obtained results revealed that thermal decomposition initiation is probably due to the scissions of methyl groups and of the oxadiazole in the side chain and the amidic group in the main chain and continues with the imide group degradation. The products eliminated during the thermal decomposition process in nitrogen atmosphere were water, carbon dioxide, benzene, methane, benzonitrile, aniline and carbon monoxide. The optical properties of the new diamine and polymers were studied by UV-vis and fluorescence spectroscopy. The absorption and fluorescence maxima were observed at 357-373 nm and 407-469 nm, respectively, depending on the structure of the compounds and the characteristics of the solvating media. The polymers showed blue fluorescence in solution, with low to moderate quantum fluorescence yields varying from 0.11 to 1.30%. Stokes shifts values were around 77 nm. The emission peaks of poly(amide-imide)s were broader than those of diamine and polyimide. Under acidic conditions the emission spectra of investigated compounds were altered.

References

[1] Sroog CE. Polyimides. Prog Polym Sci 1991;16:561-694.

[2] Sato M. Polyimides. In: Olabisi O, editor. Handbook of thermoplastics, New York: Marcel Dekker; 1997, p. 665-699.

[3] Liaw DJ, Wang KL, Huang YC, Lee KR, Lai JY, Ha CS. Advanced polyimide materials: Syntheses, physical properties and applications. Prog Polym Sci 2012;37:907-974.

[4] Vanherck K, Koeckelberghs G, Vankelecom IFJ. Crosslinking polyimides for membrane applications: A review. Prog Polym Sci 2013;38:874-896.

[5] Yi L, Huang W, Yan D. Polyimides with side groups: synthesis and effects of side groups on their properties. J Polym Sci, Part A: Polym Chem 2017;55:533-559.

[6] Liou GS, Hsiao SH, Fang YK. Electrochromic properties of novel strictly alternating poly(amine-amide-imide)s with electroactive triphenylamine moieties. Eur Polym J 2006;42:1533-1540.

[7] Shockravi A, Abouzari-Lotf E, Javadi A, Atabaki F. Preparation and properties of new *ortho*-linked polyamide-imides bearing ether, sulfur, and trifluoromethyl linkages. Eur Polym J 2009;45:1599-1606.

[8] Grabiec E, Schab-Balcerzak E, Wolinska-Grabczyk A, Jankowski A, Jarzabek B, Kozuch-Krawczyk, Kurcok M. Physical, optical and gas transport properties of new processable polyimides and poly(amide-imide)s obtained from 4,4'-[oxybis(4,1-phenylenethio)]dianiline and aromatic dianhydrides. Polym J 2011;43:621-629.

[9] Dhara MG, Banerjee S. Fluorinated high-performance polymers: Poly(arylene ether)s and aromatic polyimides containing trifluoromethyl groups. Prog Polym Sci. 2010;35:1022-1077.

[10] Ando S. Optical properties of fluorinated polyimides and their applications to optical components and waveguide circuit. J Photopolym Sci Technol 2004;17:219-232.

[11] Wozniak AI, Yegorov AS, Ivanov VS, Igumnov SM, Tcarkova KV, Recent progress in synthesis of fluorine containing monomers for polyimides. J Fluor Chem 2015;180:45-54.

[12] Vora RH, Goh SH, Chung TS. Synthesis and properties of fluoro-polyetherimides. Polym Eng Sci 2000;40:1318-1329.

[13] Lin BP, Pan Y, Qian Y, Yuan CW. Comparative study of silicon-containing polyimides from different oxydianilines. J Appl Polym Sci 2004;94:2363-2367.

[14] Schulz B, Janietz S, Sava I, Bruma M. Electrochemical characterization of thin films based on new silicon-containing aromatic poly(1,3,4-oxadiazole)s. Polym Adv Technol 1996;7:514-518.

[15] Liou GS, Huang NK, Yang YL. Synthesis, photoluminescent and electrochromic properties of new aromatic poly(amine-hydrazide)s and poly(amine-1,3,4-oxadiazole)s derived from 4,4′-dicarboxy-4″-methyltriphenylamine. Eur Polym J 2006;42:2283-2291.

[16] Kim DY, Cho HN, Kim CY. Blue light emitting polymers. Prog Polym Sci 2000;25:1089-1139.

[17] Schulz B, Bruma M, Brehmer L. Aromatic poly(1,3,4-oxadiazole)s as advanced materials. Adv Mater 1997;9: 601-613.

[18] Paun A, Hadade ND, Paraschivescu CC, Matache M. 1,3,4-Oxadiazoles as luminescent materials for organic light emitting diodes via cross-coupling reactions. Mater Chem C 2016;4:8596-8610.

[19] Krasovitskii BM, Bolotin BM. Organic luminescent materials, New York: VCH Publisher, 1988.

[20] Hamciuc C, Hamciuc E, Bruma M. New fluorinated poly(1,3,4-oxadiazole-ether-imide)s. Polymer 2005;46:5851-5859.

[21] Hamciuc C, Hamciuc E, Serbezeanu D, Vlad-Bubulac T. Thermal and optical properties of some phosphorus-containing poly(1,3,4-oxadiazole-ester-imide)s. Polym Adv Technol 2011;22:2458-2468.

[22] Hamciuc C, Hamciuc E, Cazacu M. Poly(1,3,4-oxadiazole-ether-imide)s and their polydimethylsiloxane-containing copolymers. Eur Polym J 2007;43:4739-4749.

[23] Hamciuc C, Homocianu M, Hamciuc E, Carja ID. Synthesis and photophysical study of some new highly thermostable blue fluorescent poly(1,3,4-oxadiazole-imide)s containing dimethylamine groups. React Funct Polym 2016;103:17-25.

[24] Hamciuc C, Hamciuc E, Homocianu M, Nicolescu A, Carja ID. Blue light-emitting polyamide and poly(amide-imide)s containing 1,3,4-oxadiazole ring in the side chain. Dyes Pigments 2015;114:110-123.

[25] Hamciuc E, Homocianu M, Hamciuc C, Carja ID. Synthesis and photophysical study of new blue fluorescent poly(azomethine-1,3,4-oxadiazole)s containing dimethylamino groups. High Perform Polym, DOI: https://doi.org/10.1177/0954008317697367, 2017.

[26] Hamciuc E, Bruma M, Mercer FW, Simionescu CI. Poly(benzimidazole-imide-amide)s containing hexafluoroisopropylidene units. Angew Macromol Chem 1993;210:43-150.

[27] Hamciuc E, Bruma M, Schulz B, Kopnick T. New silicon-containing poly(imide-amide)s. High Perform Polym 2003;15:347-359.

[28] Lisa G, Wilson DA, Scutaru D, Tudorachi N, Hurduc N. Investigation of thermal degradation of some ferrocene liquid crystals. Thermochim Acta 2010;507-508:49-59.

[29] Lisa G, Hamciuc C, Hamciuc E, Tudorachi N. Thermal and thermo-oxidative stability and probable degradation mechanism of some polyetherimides. J Anal Appl Pyrolysis 2016;118:144-154.

[30] Li F, Huang L, Shi Y, Jin X, Wu Z, Shen Z, Chuang KR, Lyon E, Harris FW, Cheng ZD. Thermal degradation mechanism and thermal mechanical properties of two high-performance aromatic polyimide fibers. J Macromol Sci, Part B: Physics 1999;38:107-122.

[31] Wang X, Hu Y, Song L, Xing W, Lu H, Lv P, Jie G. Flame retardancy and thermal degradation mechanism of epoxy resin composites based on a DOPO substituted organophosphorus oligomer. Polymer 2010;51:2435-2445.

[32] Alshehri SM, Ahamad T. Thermal degradation and evolved gas analysis of N,N′-bis(2-hydroxyethyl) linseed amide (BHLA) during pyrolysis and combustion. J Therm Anal Calorim 2013;114:1029-1037.

[33] Szczesny R, Szłyk E. Thermal decomposition of some silver (I) carboxylates, under nitrogen atmosphere. J Therm Anal Calorim 2013;111:1325-1330.

[34] Nistor MT, Vasile C. TG/FTIR/MS study on the influence of nanoparticles content upon the thermal decomposition of starch/poly(vinyl alcohol) montmorillonite nanocomposites. Iran Polym J 2013;22:519-536.

[35] Spiliopoulos IK, Mikroyannidis JA, Tsivgoulis GM. Rigid-rod polyamides and polyimides derived from 4,3″-diamino-2′,6′-diphenyl- or di(4-biphenylyl)-p-terphenyl and 4-amino-4″-carboxy-2′,6′-diphenyl-p-terphenyl and 4-amino-4″-carboxy-2′,6′-diphenyl-p-terphenyl Macromolecules 1998;31:522-529.

[36] Zhanga C, Renb Z, Liu L, Yin Z. Modelling hydrogen bonds in N, N-dimethylformamide. Mol Simul 2013;39:875-881.

[37] Ding L, Karasz FE, Lin Y, Pang Y, Liao L. Photoluminescence and electroluminescence study of violet-blue and green emitting polymers and their blend. Macromolecules 2003;36:7301-7307.

[38] Sasireka V, Ramakrishnan V. Study of preferential solvation of 2,6-diaminoanthraquinone in binary mixtures by absorption and fluorescence studies. Spectrochim Acta Part A 2008;70:626-633.

[39] Grante I, Actins A, Orola L. Protonation effects on the UV/Vis absorption spectra of imatinib: A theoretical and experimental study. Spectrochim Acta Part A: Molec Biomol Spectrosc 2014;129: 326–332.

Figure captions

Scheme 1. Synthesis of diamine **7**.

Scheme 2. The proposed thermal degradation mechanism for **10b**.

Fig. 1. ^{1}H NMR spectrum of diamine **7**.

Fig. 2. Chemical structure of poly(amide-imide)s **10a**, **10b**, **10c**, and polyimide **11.**

Fig. 3. ^{1}H NMR spectrum of **10a**.

Fig. 4. DTG curves of polymers **10** and **11**.

Fig. 5. Ionic current variation with temperature for the fragments: m/z = 15 (a), m/z = 103 and 93 (b), m/z = 78 (c) and m/z = 30 (d), for **10b**.

Fig. 6. FTIR spectra of the volatile products evolved during thermal decomposition of **10b**.

Fig. 7. UV-Vis absorption spectra for the all investigated polymers in DMF solution (a) and for poly(amide-imide) **10a** in selected solvents (b).

Fig. 8. Fluorescence spectra of all investigated samples in DMF solution (a) and of poly(amide-imide) **10b** in selected solvents (b), the CIE 1931 (X,Y) chromaticity diagram of all investigated compounds in dilute DMSO solution (c).

Fig 9. The emission spectra for **10b** in DMAc solution (a) and diamine **7** in DMF solution (b) with an increase of excitation wavelength from 363 to 415 nm.

Fig. 10. Changes in the UV-Vis absorption (a) and emission spectra (b) of **10a** upon the addition of dilute solution of HCl.

Scheme 1

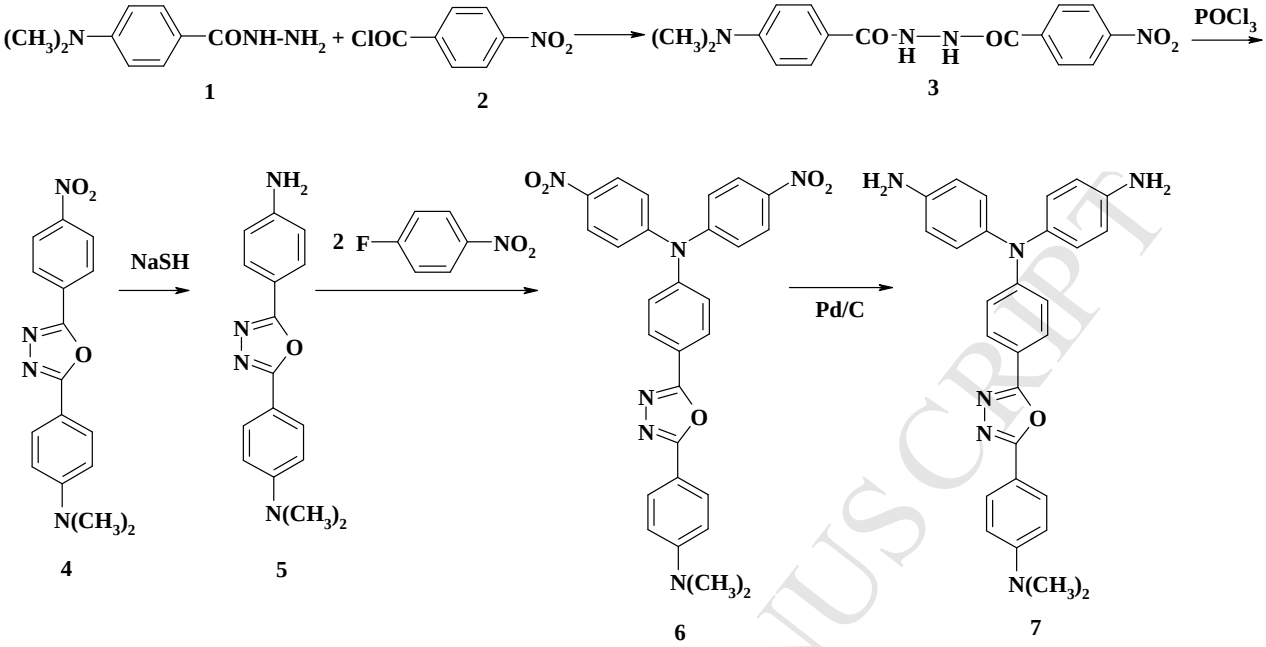

Scheme 2

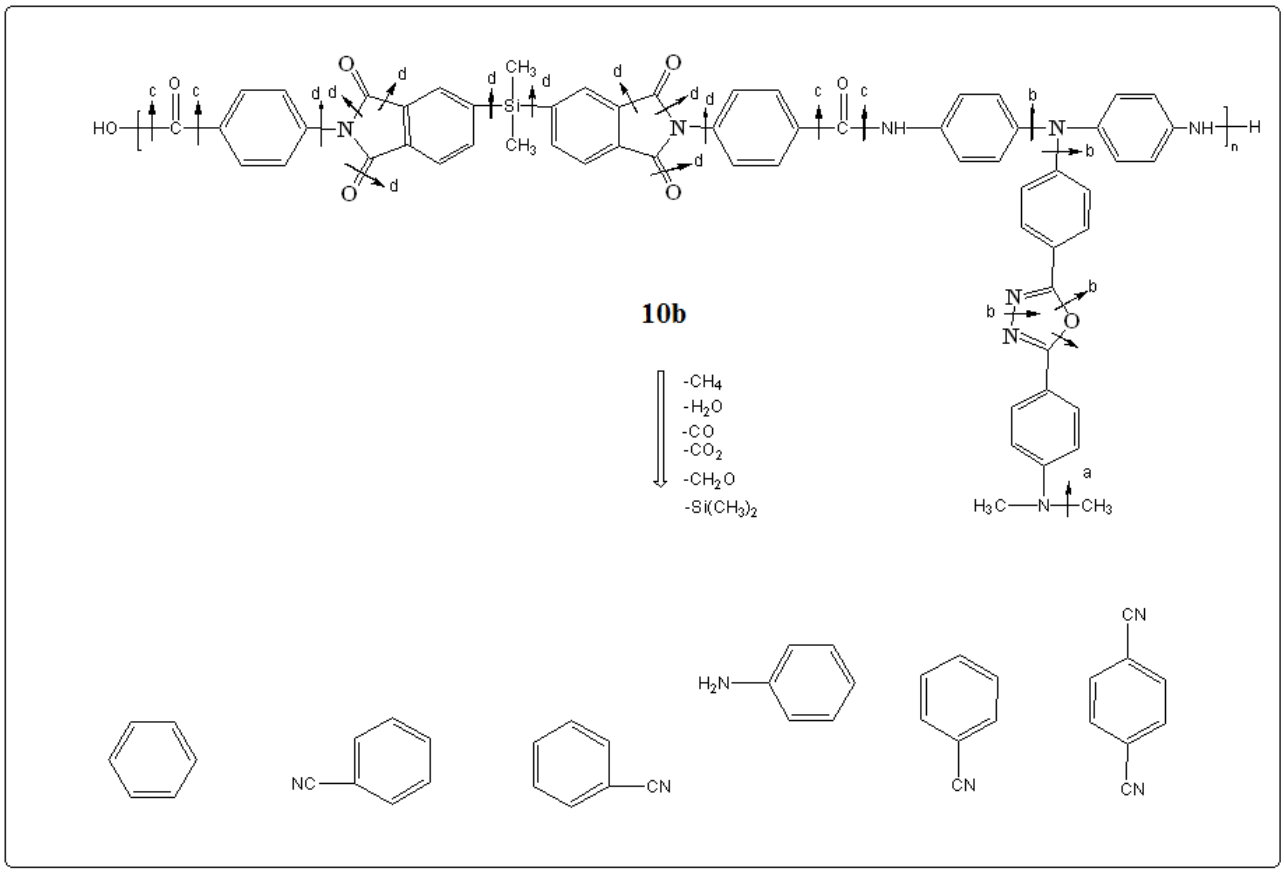

Figure 1

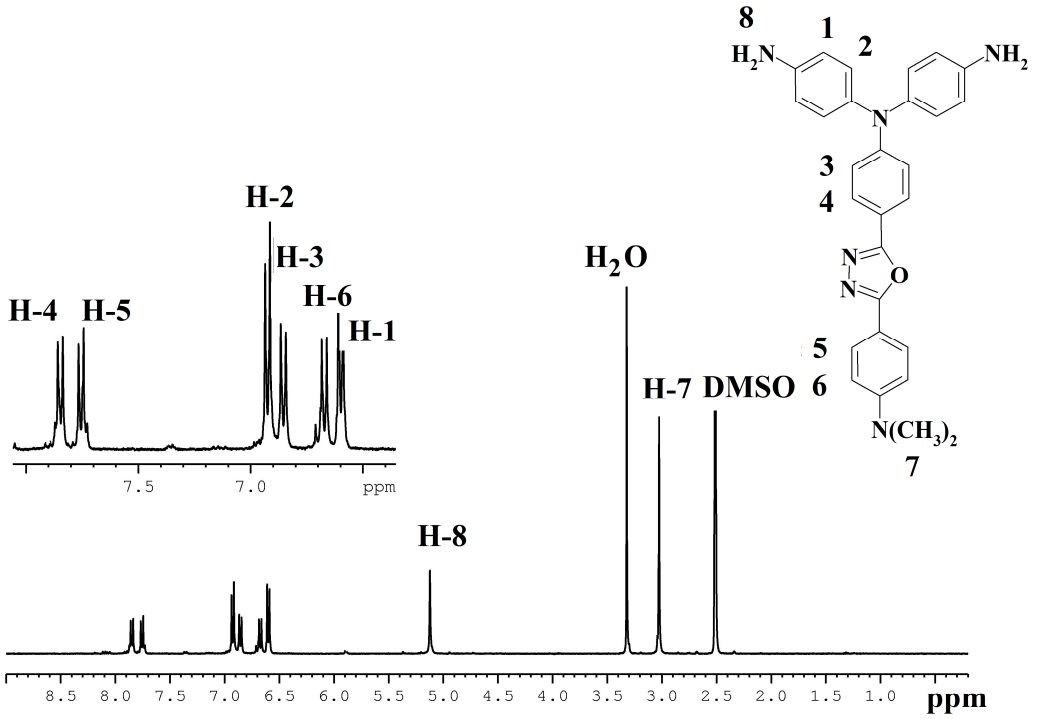

Figure 2

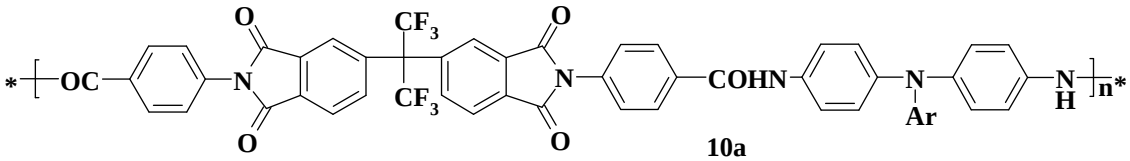

10a

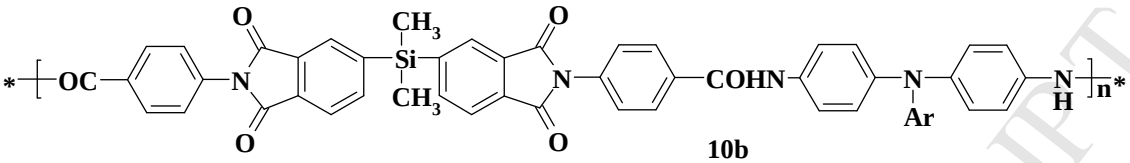

10b

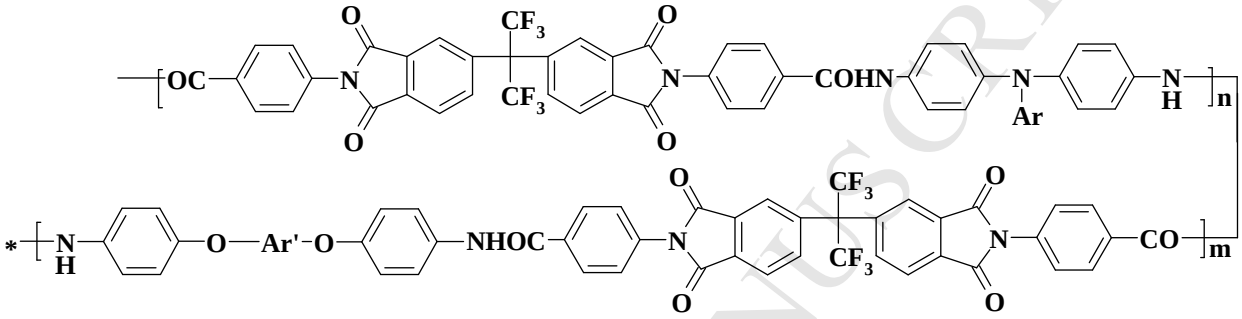

10c

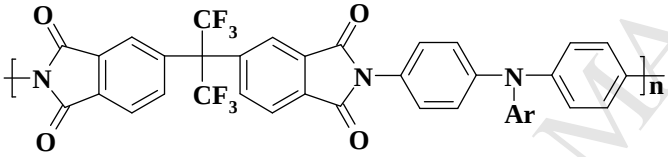

11

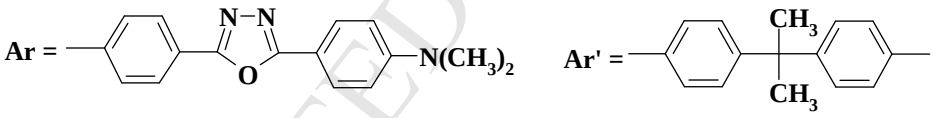

Figure 3

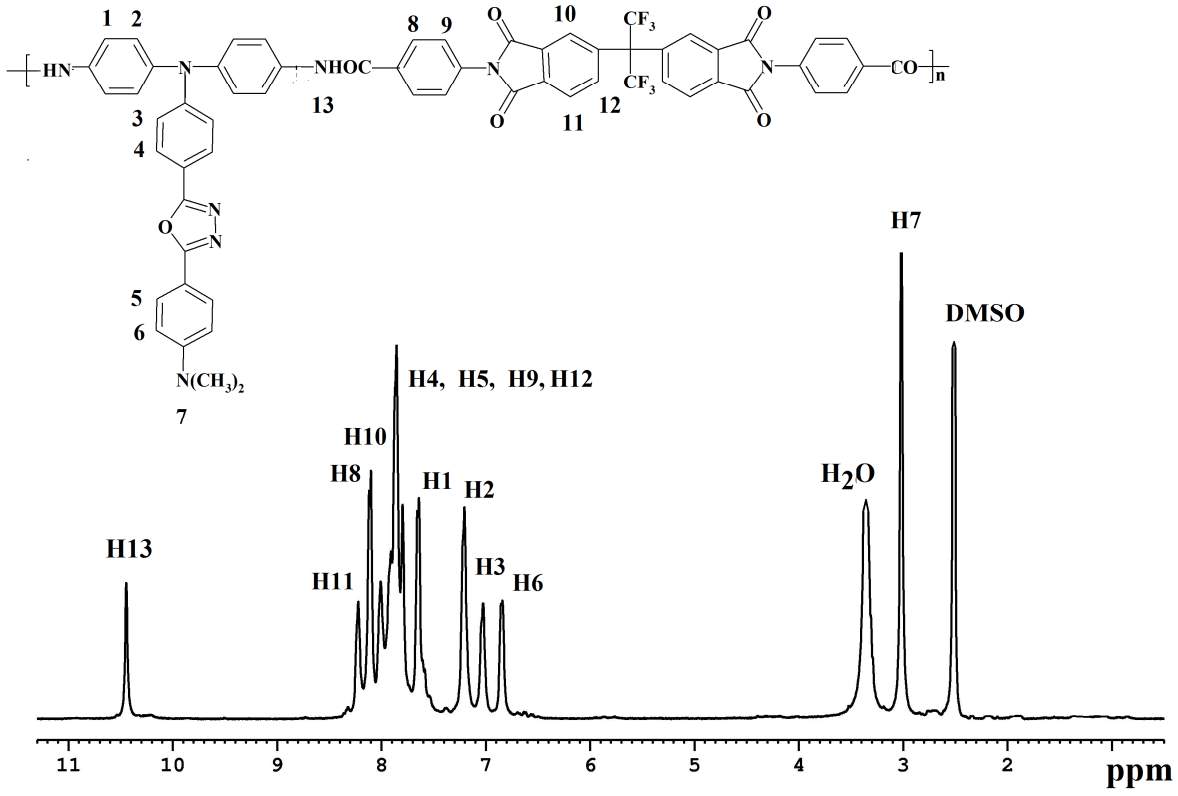

Figure 4

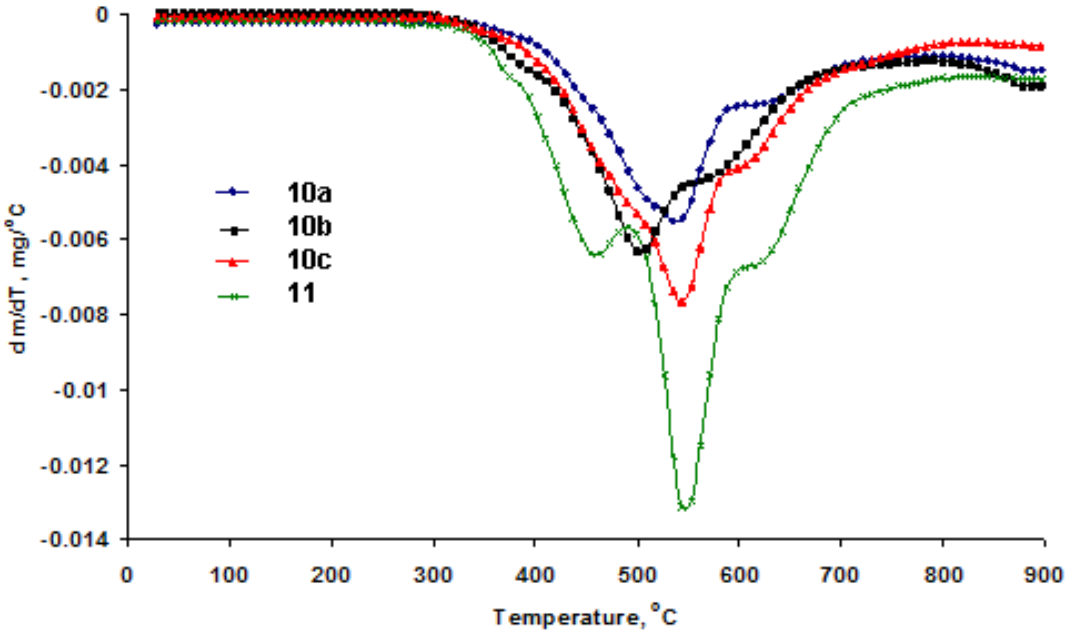

Figure 5

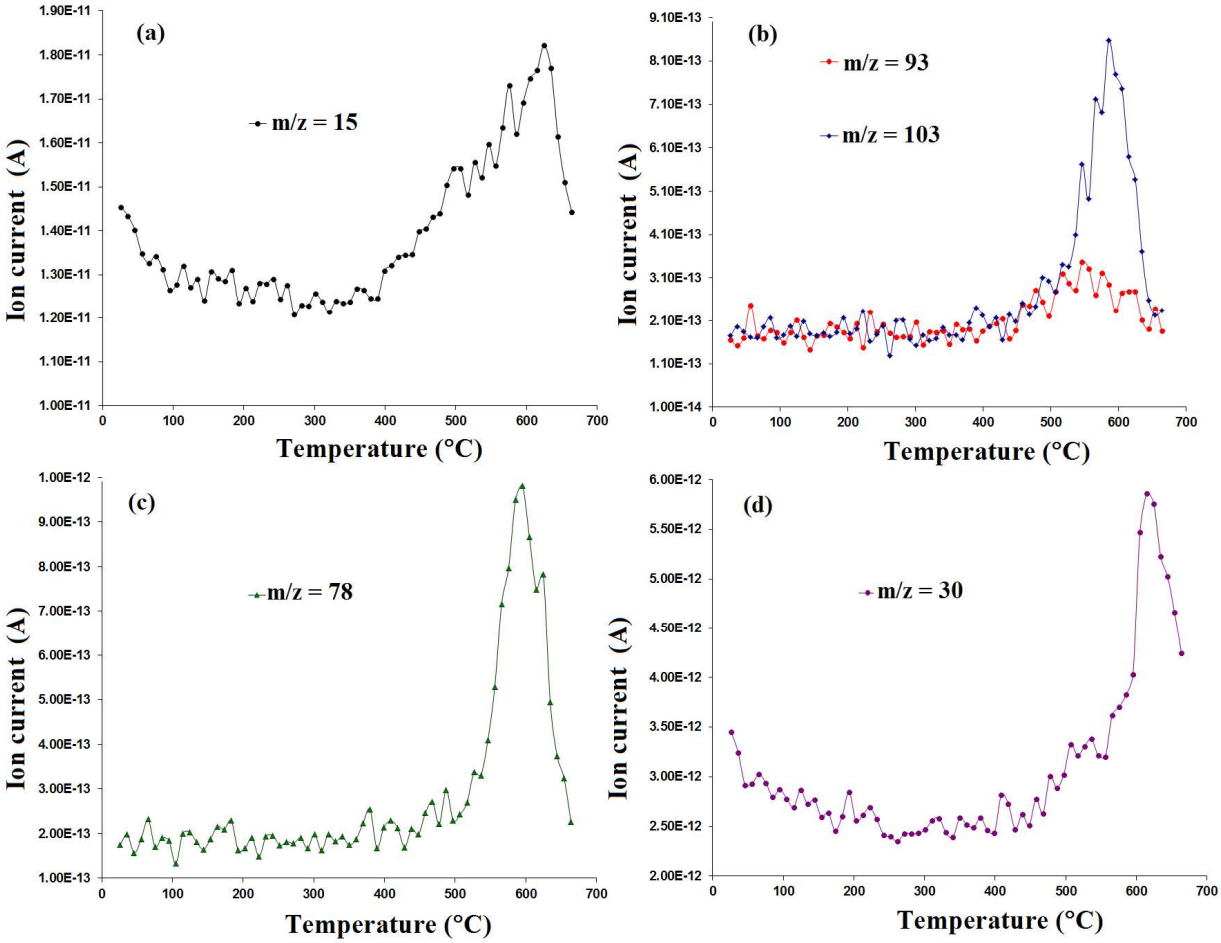

Figure 6

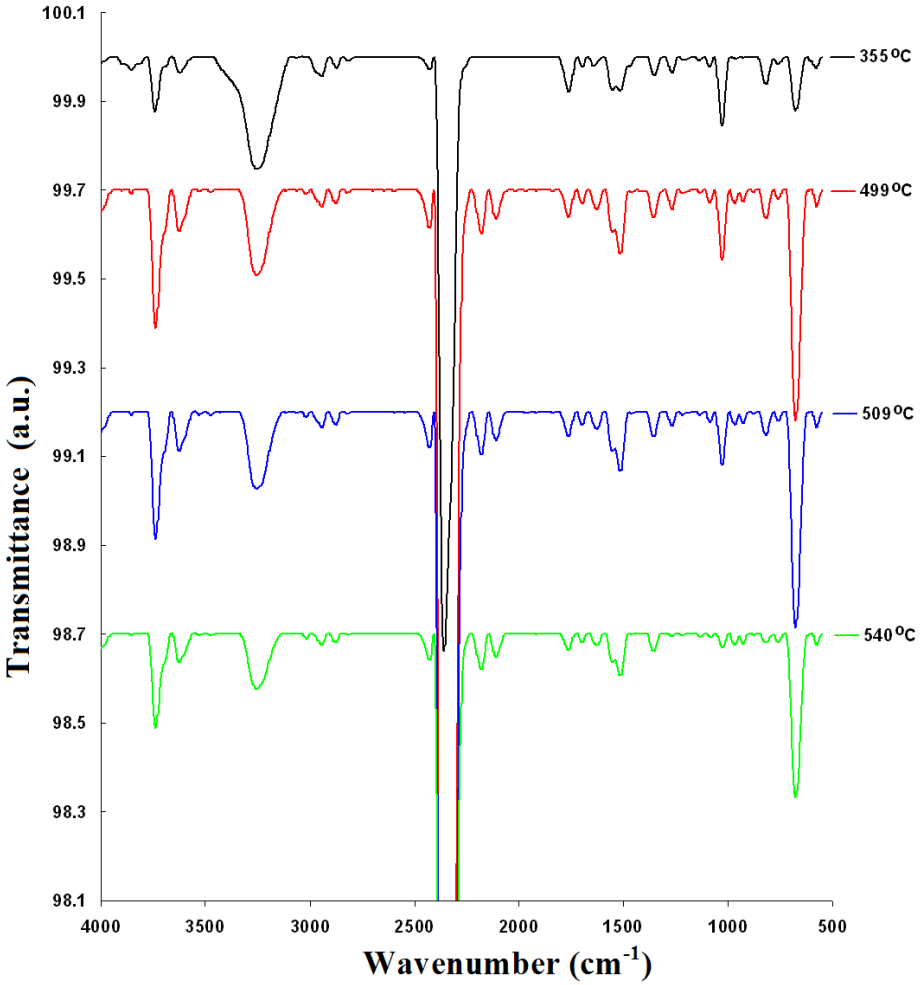

Figure 7

(a)

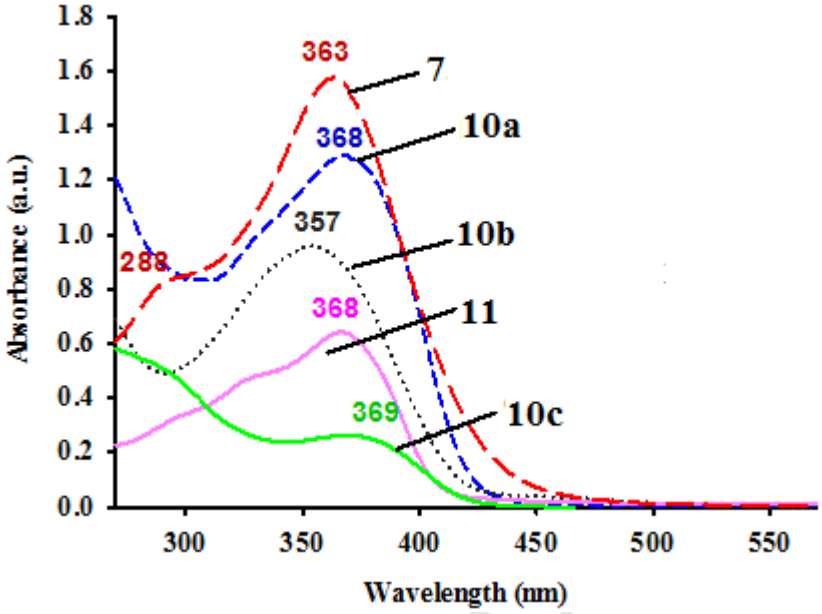

(b)

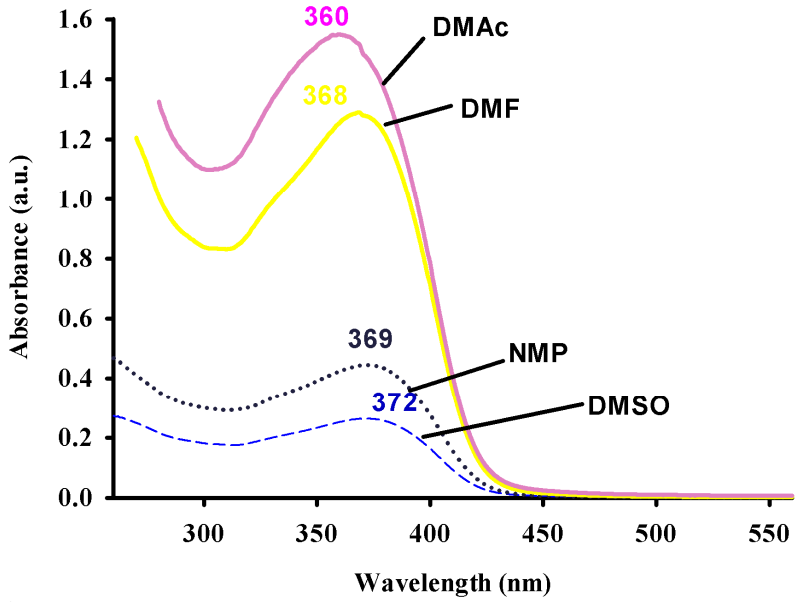

Figure 8

(a)

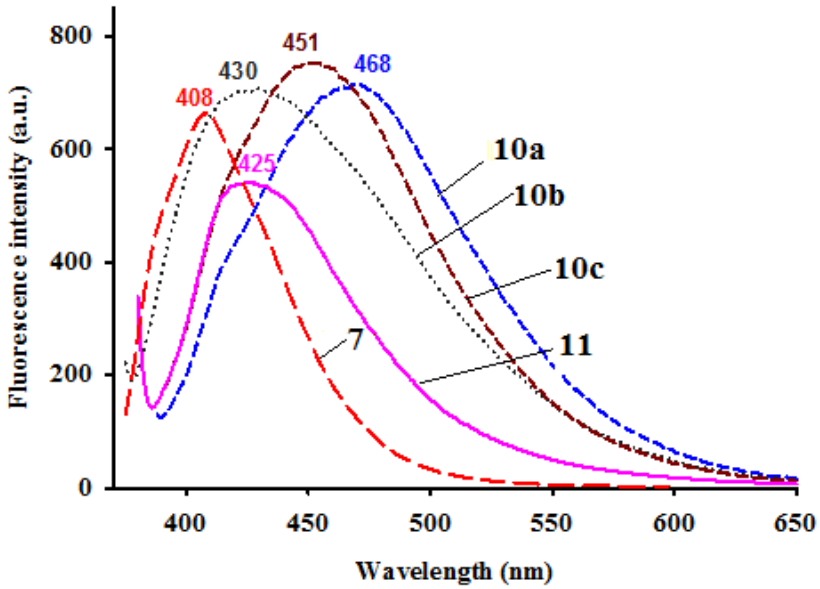

(b)

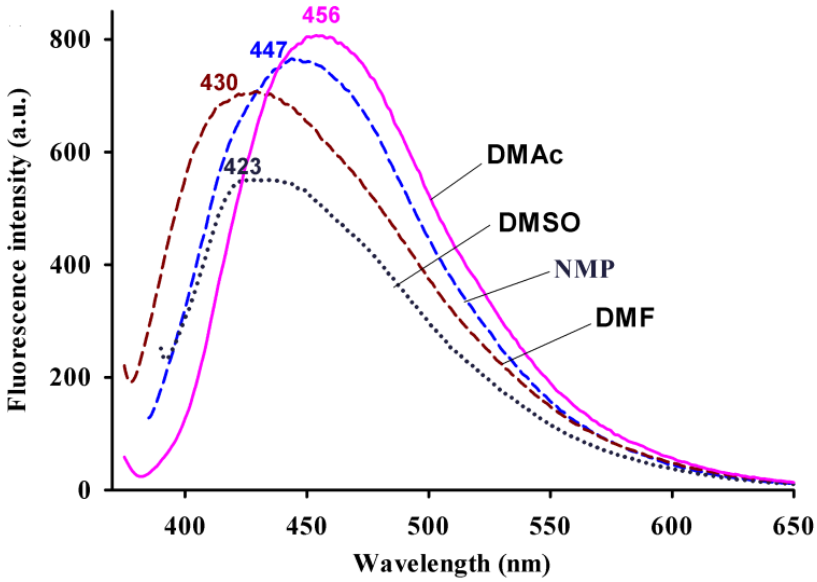

(c)

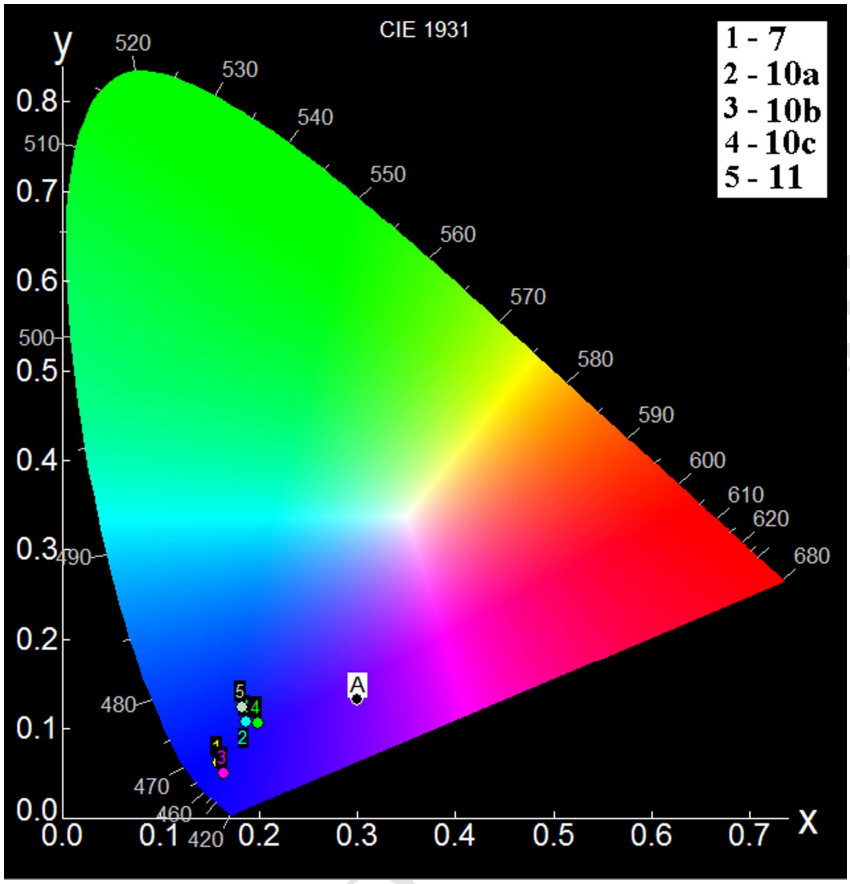

Figure 9

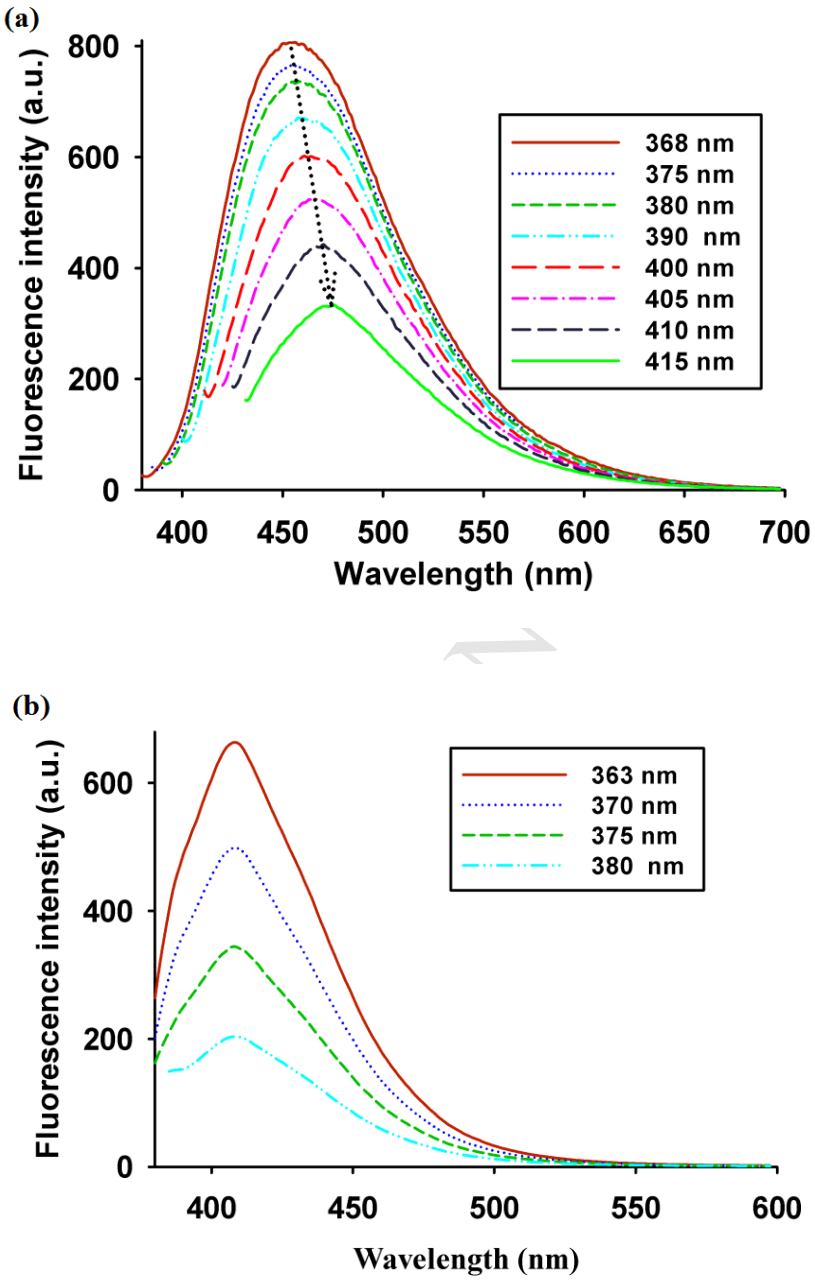

Figure 10

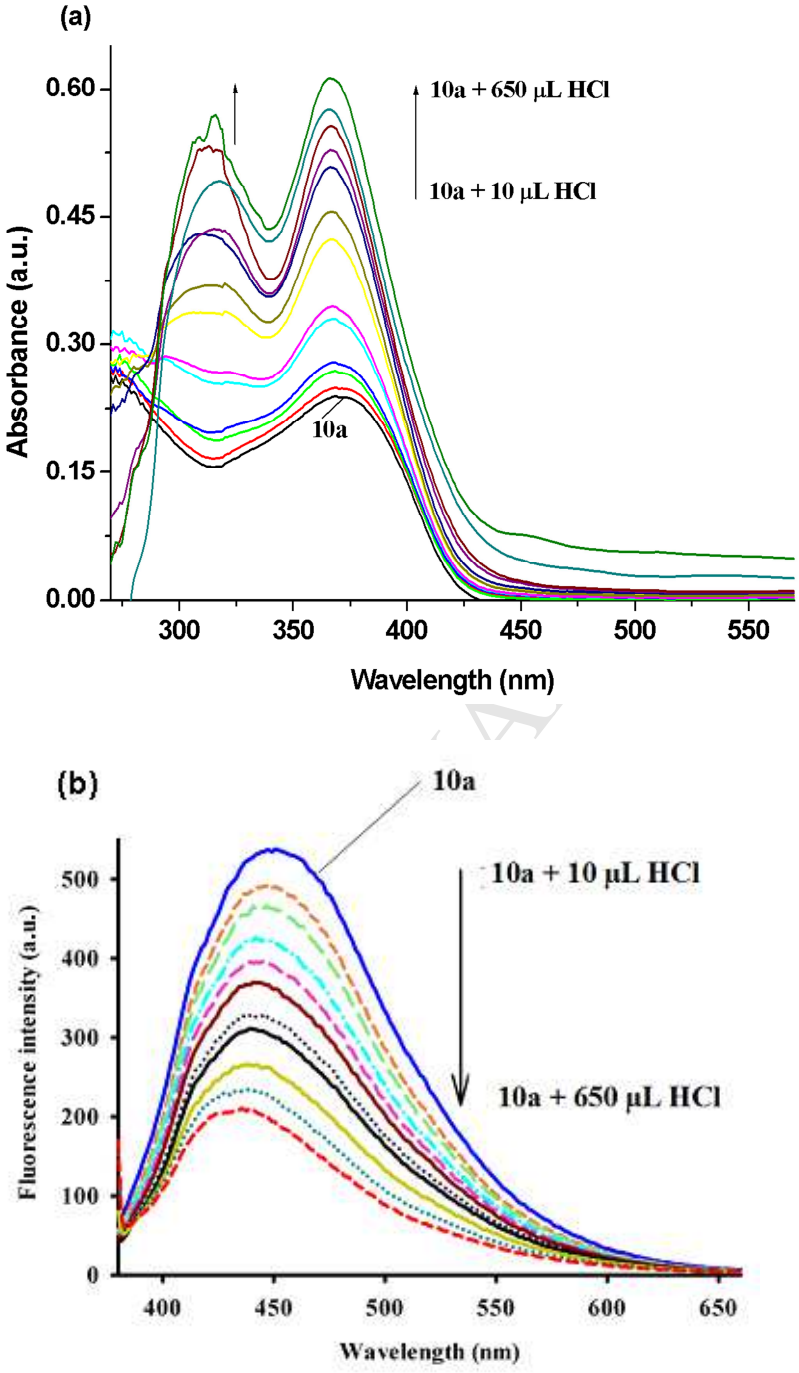

Table 1

Thermogravimetric characteristics of the polymers.

Polymer	Stage	T_{Onset} [a] (°C)	T_{Peak} [b] (°C)	T_{Endset} [c] (°C)	W[d] (%)	M_{Resid} [e] (%)
10a	I	442	541	579	27.47	51.24
	II	579	624	721	21.29	
10b	I	381	503	540	22.43	50.93
	II	540	572	721	26.64	
10c	I	441	543	561	23.56	57.84
	II	561	601	701	18.60	
11	I	396	458	524	15.30	53.23
	II	524	548	570	10.37	
	III	570	618	700	21.10	

[a] The onset temperature of the decomposition.

[b] Thermal degradation peak temperature of the decomposition process.

[c] The end set temperature of the decomposition.

[d] Mass loss in every stage.

[e] Weight loss after the end of decomposition process.

Table 2

The values of maxima at the highest wavelength absorption bands (λ_{abs}) and emission bands (λ_{em}), Stokes shifts (SS), the full width at half-maximum of the emission band ($FWHM_{em}$) and emission quantum yields (QY) values for investigated samples (c = 1.57×10^{-5} mol L^{-1}), in selected solvents.

Compound	Media	λ_{abs} (nm)	λ_{em} (nm)	SS (nm)	$FWHM_{em}$ (nm)	QY (%)
7	NMP	288^{sh}, 366	409	43	64	-
	DMF	288^{sh}, 363	408	45	64	-
	DMAc	288^{sh}, 363	407	44	60	-
	DMSO	288^{sh}, 364	412	48	62	8.28
10a	NMP	369	444	75	107	-
	DMF	368	468	100	117	-
	DMAc	360	455	95	89	-
	DMSO	372	469	92	114	0.11
10b	NMP	373	447	74	105	-
	DMF	357	429	72	115	-
	DMAc	368	456	88	100	-
	DMSO	373	423	50	107	0.88
10c	NMP	369	446	77	103	-
	DMF	369	451	82	106	-
	DMAc	369	451	82	97	-
	DMSO	373	452	79	106	0.18
11	NMP	368	439	42	80	-

DMF	367	425	40	64	-
DMAc	367	422	41	62	-
DMSO	369	417	43	64	1.30

[sh]-shoulder.

Supplementary material

New blue fluorescent and highly thermostable polyimide and poly(amide-imide)s containing triphenylamine units and (4-dimethylaminophenyl)-1,3,4-oxadiazole side groups

Corneliu Hamciuc[1], Elena Hamciuc[1], Mihaela Homocianu[1], Gabriela Lisa[2]

[1]"Petru Poni" Institute of Macromolecular Chemistry, 41A Aleea Gr. Ghica Voda, 700487 Iasi, Romania

[2]"Gheorghe Asachi" Technical University of Iasi, Faculty of Chemical Engineering and Environmental Protection, Department of Chemical Engineering, 73 D. Mangeron Street, Iasi, Romania

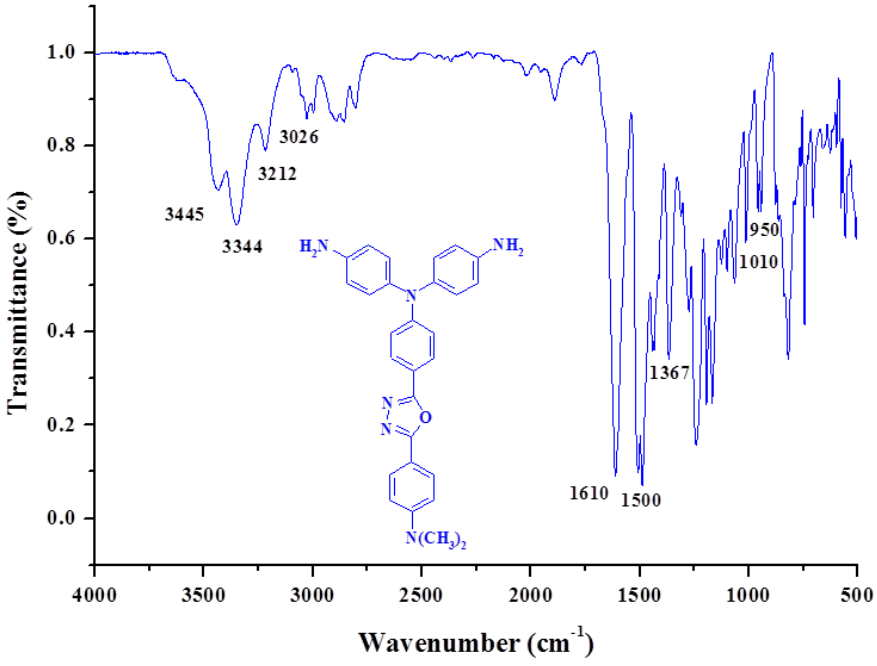

Fig. S1. FTIR spectrum of diamine **7**.

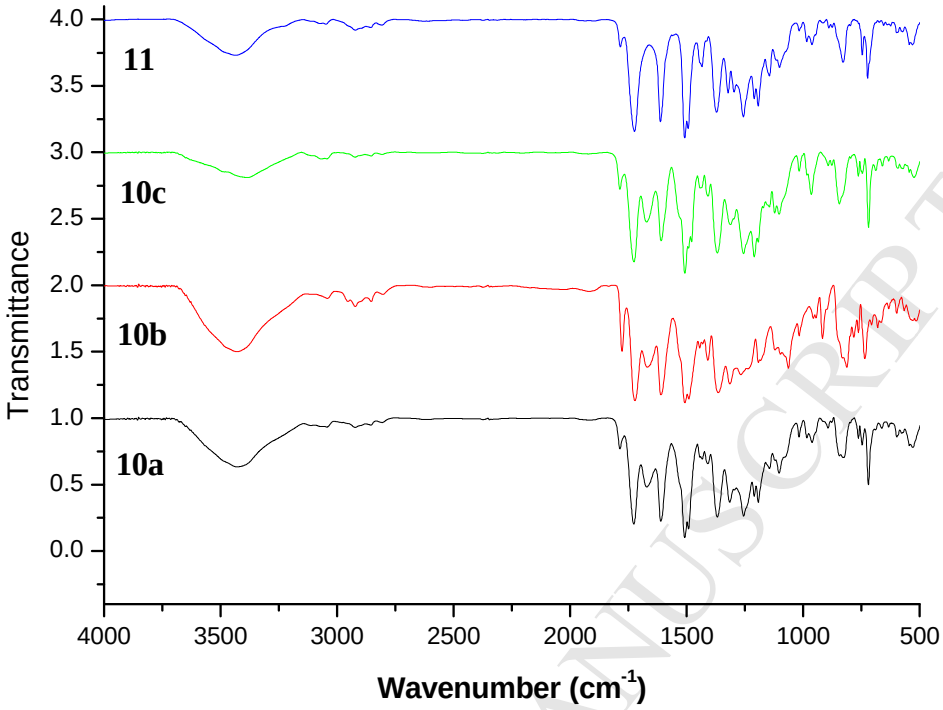

Fig. S2. FTIR spectra of the polymers.

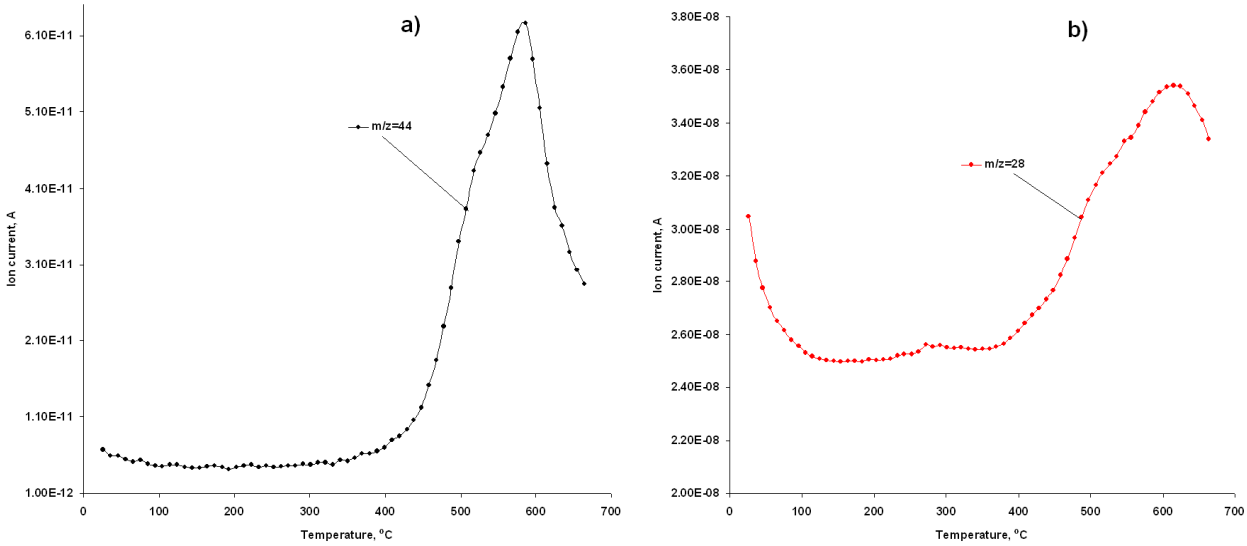

Fig. S3. Ionic current variation with temperature for the fragments: m/z = 44 (a) and m/z = 28 (b).

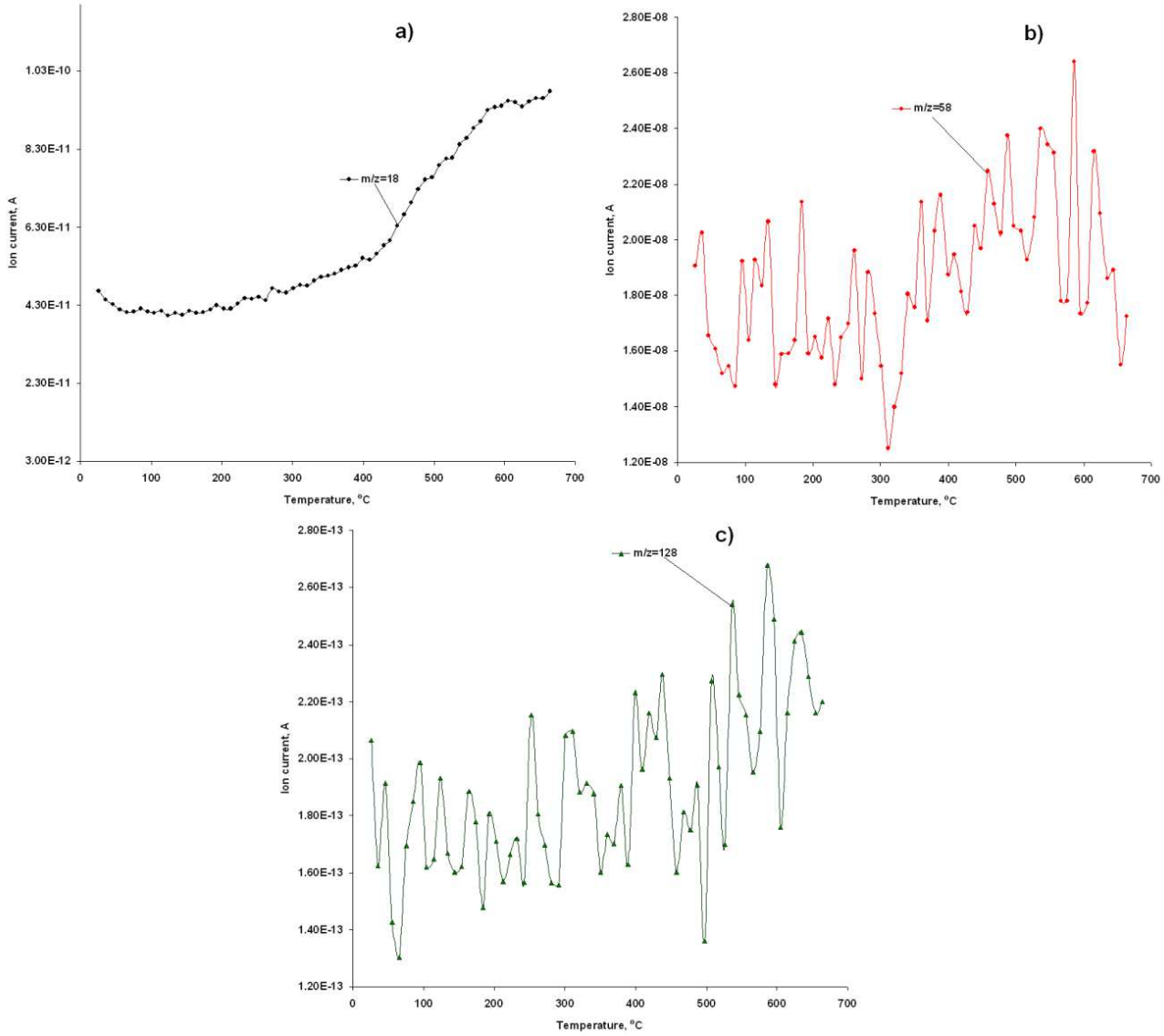

Fig. S4. Ionic current variation with temperature for the fragments: m/z = 18 (a), m/z = 58 (b) and m/z = 128 (c).

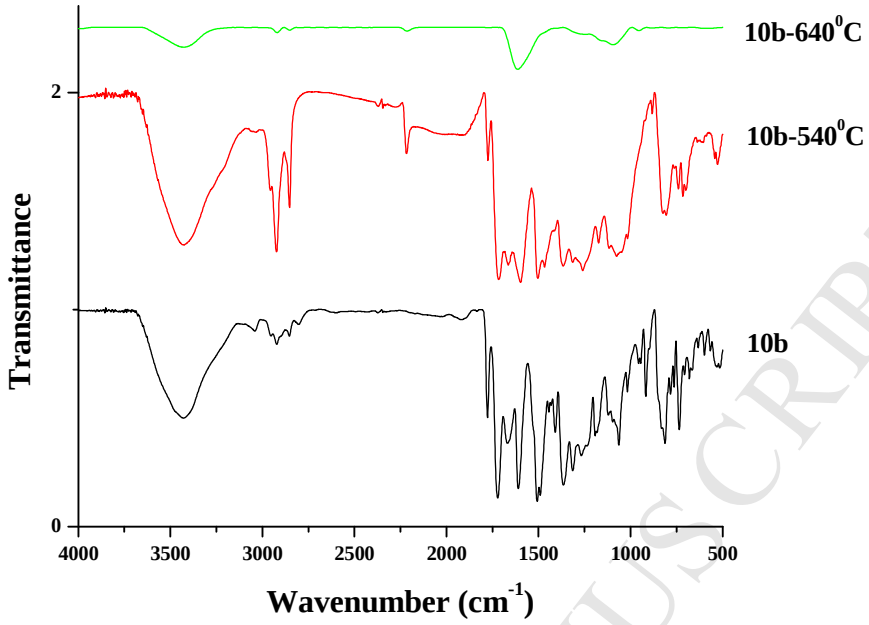

Fig. S5. FTIR spectra of **10b** and of **10b** heated up to 540°C and 640°C with the heating rate of 10°C min^{-1}, in nitrogen atmosphere.

Highlights

1. A new blue fluorescent diamine having a triphenylamine group and 1,3,4-oxadiazole ring was synthesized;
2. Highly thermostable aromatic polyimide and poly(amide-imide)s with blue fluorescent properties were prepared;
3. A thermal decomposition study was performed;
4. The fluorescence characteristics were determined in solution using different solvents;
5. The fluorescence quenching process was studied in the presence of hydrochloric acid.